Technical Report Documentation Page

1. Report No.	2. Government Accession No.	3. Recipient's Catalog No.
FHWA/TX-07/9-1502-01-8		

4. Title and Subtitle	5. Report Date
DEVELOPMENT AND VERIFICATION OF THE OVERLAY TESTER BASED FATIGUE CRACKING PREDICTION APPROACH	September 2006 Published: January 2007
	6. Performing Organization Code

7. Author(s)	8. Performing Organization Report No.
Fujie Zhou, Sheng Hu, and Tom Scullion	Report 9-1502-01-8

9. Performing Organization Name and Address	10. Work Unit No. (TRAIS)
Texas Transportation Institute The Texas A&M University System College Station, Texas 77843-3135	11. Contract or Grant No. Project 9-1502-01

12. Sponsoring Agency Name and Address	13. Type of Report and Period Covered
Texas Department of Transportation Research and Technology Implementation Office P. O. Box 5080 Austin, Texas 78763-5080	Technical Report: September 2005-August 2006
	14. Sponsoring Agency Code

15. Supplementary Notes

Project performed in cooperation with the Texas Department of Transportation and the Federal Highway Administration.

Project Title: Model Calibrations with Local APT Data and Implementation for Focus on Solutions to NAFTA Problems

URL: http://tti.tamu.edu/documents/9-1502-01-8.pdf

16. Abstract

Fatigue cracking is one of the major distress modes in the long-term performance of asphalt pavements. Many research efforts have been made to study the fatigue behavior of asphalt pavements. Various fatigue analysis approaches have been developed, and some are in use today. However, many approaches (or models) are inaccurate in predicting fatigue performance of asphalt pavements. Consequently, fatigue cracking prediction continues to be a major concern for pavement engineers.

The main objective of this project was to develop and verify the overlay tester (OT) based fatigue cracking prediction approach in which the OT is used to determine fracture properties (A and n) of hot-mix asphalt (HMA) mixtures. This approach was developed based on fracture mechanics. However, not only was the fatigue crack propagation characterized by Paris' law fracture concepts, but the crack initiation described by traditional fatigue model was also included in this approach. In this approach, the fundamental HMA fracture properties (A and n) were used to estimate fatigue life of asphalt pavements including crack initiation and crack propagation. Note that the traditional fatigue (crack initiation) model parameters, k_1 and k_2, were also estimated from the fracture properties (A and n) through the quantitative relationship that was established based on theoretical investigation and historical bending beam fatigue test data (1348 data sets). Field verification of this OT based fatigue crack prediction approach was demonstrated with performance data collected from the Federal Highway Administration's Accelerated Loading Facility (FHWA-ALF) test program. The proposed approach has been successfully verified by analyzing five FHWA-ALF fatigue test lanes. The ranking of the predicted fatigue life for the ALF test lanes had a very good agreement with the measured fatigue performance data under the ALF loading. However, further field validation using other data sets is still needed.

17. Key Words	18. Distribution Statement
Overlay Tester, Fatigue Cracking, FHWA-ALF, Crack Initiation, Crack Propagation	No restrictions. This document is available to the public through NTIS: National Technical Information Service Springfield, Virginia 22161 http://www.ntis.gov

19. Security Classif.(of this report)	20. Security Classif.(of this page)	21. No. of Pages	22. Price
Unclassified	Unclassified	90	

DEVELOPMENT AND VERIFICATION OF THE OVERLAY TESTER BASED FATIGUE CRACKING PREDICTION APPROACH

by

Fujie Zhou
Assistant Research Engineer
Texas Transportation Institute

Sheng Hu
Associate Transportation Researcher
Texas Transportation Institute

and

Tom Scullion
Research Engineer
Texas Transportation Institute

Report 9-1502-01-8
Project Number 9-1502-01
Project Title: Model Calibrations with Local APT Data and Implementation for Focus on Solutions to NAFTA Problems

Performed in cooperation with the
Texas Department of Transportation
and the
Federal Highway Administration

September 2006
Published: January 2007

TEXAS TRANSPORTATION INSTITUTE
The Texas A&M University System
College Station, Texas 77843-3135

DISCLAIMER

The contents of this report reflect the views of the authors, who are responsible for the facts and the accuracy of the data presented herein. The contents do not necessarily reflect the official views or policies of the Texas Department of Transportation or the Federal Highway Administration. The United States Government and the State of Texas do not endorse products or manufacturers. Trade or manufacturers' names appear herein solely because they are considered essential to the object of this report. This report does not constitute a standard, specification, or regulation. The engineer in charge was Tom Scullion, P.E. (Texas, # 62683).

ACKNOWLEDGMENTS

This work was completed as part of a pooled-fund project entitled "Model Calibrations with Local APT Data and Implementation for Focus on Solutions to NAFTA Problems." The states of Texas, Louisiana, and New York provided funds for this project. The technical representatives are Dr. Dar-Hao Chen (Texas), Dr. Julian Bendana (New York), and Mr. Marsood Rasoulian (Louisiana). Their guidance throughout this project is acknowledged and greatly appreciated.

Special thanks go out to Dr. Nelson H. Gibson and Dr. Imad Basheer, Federal Highway Administration, for coordinating and shipping the cores to TTI. Additional recognition goes out to Dr. Ghazi Al-Katheeb of SaLUT Inc., Turner-Fairbank Highway Research Center for providing the dynamic modulus data. Appreciation is highly expressed to Dr. Bor-Wen Tsai, Prof. Carl L. Monismith, UC-Berkeley; Mr. Robert Staugaard, Secretary of the Pacific Coast Conference on Asphalt Specifications; and Dr. Jorge B. Sousa, Consulpav International for providing the bending beam fatigue test results.

TABLE OF CONTENTS

Page

TABLE OF CONTENTS (CONTINUED)

Page

LIST OF FIGURES

Figure **Page**

LIST OF FIGURES (CONTINUED)

Figure **Page**

LIST OF TABLES

Table **Page**

CHAPTER 1
INTRODUCTION

BACKGROUND

Fatigue cracking is one of the major distress modes in the long-term performance of asphalt pavements. Many research efforts have been made to study the fatigue behavior of asphalt pavements. Various fatigue analysis approaches have been developed, and some are in use today. For example, the Mechanistic-Empirical Pavement Design Guide (MEPDG) produced under the National Cooperation Highway Research Project (NCHRP) 1-37A used the traditional fatigue cracking prediction approach (*1*). Additionally, to validate and/or verify the fatigue cracking model or others, field experimental road or accelerated pavement tests have been constructed, such as the Federal Highway Administration – Accelerated Load Facility (FHWA-ALF) fatigue tests in McLean, VA. However, many approaches (or models) are inaccurate in predicting fatigue performance of asphalt pavements. Consequently, fatigue cracking prediction continues to be a major concern for pavement engineers.

It is well known that fatigue cracking is not simply a material problem, but is also highly related to pavement structure, traffic loading (speed, level, and volume), asphalt binder aging, and environmental conditions. Therefore, comprehensive fatigue analysis approaches that take into account the complex nature of hot-mix-asphalt (HMA) mixtures, pavement structure, traffic, environment, and other factors are needed to better predict fatigue performance of asphalt pavements. Fatigue cracking models associated with such approaches should have the potential to utilize fundamental HMA mixture properties. Furthermore, it is desirable to obtain these fundamental material properties from simple routine laboratory tests rather than time-consuming fatigue tests. This project was conducted at the Texas Transportation Institute (TTI) to develop such an approach called the overlay tester (OT) based fatigue cracking prediction approach.

RESEARCH OBJECTIVES

Two major objectives of this project are summarized below:

- verification of the MEPDG fatigue cracking model using the FHWA-ALF fatigue test results
- development and verification of the OT based fatigue cracking prediction approach in which the OT is used to characterize fracture properties of HMA mixtures (A and n).

RESEARCH APPROACH

The research approach used in this project to achieve the above objectives includes the following steps:

1. Verify the MEPDG fatigue cracking model using the FHWA-ALF fatigue test data.
2. Develop a methodology for determining HMA fracture properties (A and n) from the OT.
3. Propose a new fatigue cracking prediction approach in which the fracture properties (A and n) determined from the OT are used to estimate both the number of load repetitions required to form a macro-crack from micro-cracks (crack initiation stage) and the number of load repetitions needed for the macro-crack to penetrate the asphalt layer (crack propagation stage). This approach was developed based on fracture mechanics. The fundamental HMA fracture properties (A and n) were used to estimate fatigue life of asphalt pavements. However, not only is the fatigue crack propagation considered, but the crack initiation (the number of load repetitions required to form a macro-crack from micro-cracks) is also included in this approach. Therefore, the approach proposed in this project is different from traditional fatigue crack approaches (such as the fatigue models used in the MEPDG) in which the fatigue crack propagation stage is not directly considered; it is also different from the often used fracture mechanics approaches in which the fatigue crack initiation stage is often ignored.
4. Verify and/or demonstrate the proposed fatigue cracking prediction approach, with a focus on results obtained from the FHWA-ALF fatigue tests.

REPORT ORGANIZATION

This report is organized into five chapters. Chapter 1 presents a brief introduction. Chapter 2 documents the FHWA-ALF fatigue tests including the falling weight deflectometer (FWD) data and laboratory dynamic modulus test on HMA layer. The verification of the MEPDG fatigue cracking model is discussed in Chapter 3. Chapter 4 describes the OT based fatigue cracking prediction approach in which its development, verification, and demonstration are presented. Finally, Chapter 5 provides findings and conclusions of this project.

CHAPTER 2
FHWA-ALF FATIGUE TESTS

BACKGROUND

With the increasing use of polymer-modified asphalt binders, the limitations of current Superpave's asphalt binder performance grade (PG) specifications have been widely discussed. Under current PG specifications, the rankings of many polymer-modified asphalt binders by standardized laboratory test procedures were not consistent with what have been observed in the field. Then, the FHWA launched a multiyear effort to study the performance of Superpave mixtures containing polymer-modified asphalt binders. This research was supported by 16 state highway agencies and more than 30 industry sponsors through a transportation pooled-fund study TPF-5 (019) titled, "Full-Scale Accelerated Performance Testing for Superpave and Structural Validation," in which the Texas Department of Transportation participated. In the summer of 2002, 12 full-scale lanes of pavements with various modified asphalt binders were constructed at the FHWA's Pavement Test Facility in Virginia. In December 2002, loading began on the pavements using two ALF machines to induce two primary modes of failure: rutting and fatigue cracking. However, only fatigue cracking is discussed here, since this project focused only on fatigue cracking.

FHWA-ALF FATIGUE TESTS AND RESULTS

Pavement Structures and Materials

The layout of the 12 as-built pavement lanes is presented in Figure 1 (*2*). All pavement lanes consist of an HMA layer and a dense-graded, crushed aggregate base (CAB) course over a uniformly prepared, AASHTO A-4 subgrade soil. The total thickness of the HMA and CAB layers is 660 mm. Lanes 1 through 7 were constructed with a 4 inch (100 mm) thick layer of HMA mix, while lanes 8 though 12 were constructed with a 6 inch (150 mm) thick layer of HMA mix. The binders used in each lane are also listed in Figure 1. Note that the control binder (PG 70-22) and three modified binders (Air-Blown, SBS-LG, and Terpolymer) were used in both 4 inch (100 mm) and 6 inch (150 mm) thick lanes. All the asphalt layer for each test lane were constructed in two lifts, each 2 inches (50 mm) or 3 inches (75 mm) thick, as appropriate.

CR-AZ = Crumb rubber asphalt binder, Arizona Department of Transportation (DOT) wet process

PG 70-22 = Unmodified asphalt binder control

Air Blown = Air-Blown asphalt binder

SBS LG = Styrene-Butadiene-Styrene modified asphalt binder with linear grafting

CR-TB = Crumb rubber asphalt binder, Terminal Blend

Terpolymer = Ethylene Terpolymer modified asphalt binder

Fiber = Unmodified PG 70-22 asphalt binder with 0.2 percent polyester fiber by mass of the aggregate

SBS 64-40 = Styrene-Butadiene-Styrene modified asphalt binder graded PG 64-40

Figure 1. Layout of the 12 As-Built Pavement Lanes (*2*).

Materials

Asphalt Binders

Most of the binders chosen for this field project had the same base asphalt (a Venezuelan blend) and were modified to have the same high temperature Superpave performance grade (PG 74-xx) so that the observed performance could be attributed only to the mode of modification. Testing of binder samples collected during construction showed that the binders had the following continuous PG values: PG 70-22 control (continuous PG 72-23); air-blown (PG 74-28); SBS LG (PG 74-28); CR-TB (PG 79-28); Terpolymer (PG 74-31); and SBS 64-40 (PG 71-28). The CR-TB missed the PG target of 74-xx, and the SBS 64-40 was purposely

designed to have a PG different from the rest in order to check out whether the performance of binders with high polymer content and soft bases can be captured by the Superpave specification. The intermediate grade temperatures for $|G^*|\sin\delta = 5$MPa, which are shown in the legend of Figure 2, differ significantly and should provide a good test for checking the ability of the current intermediate binder specification to rate asphalt binders according to the fatigue cracking performance (*3*).

Aggregates and HMA Gradations

Two aggregate gradations were used in the HMA mixes, as shown in Table 1. Gradation A, which consisted of 100 percent crushed diabase stone with a 0.5 inch (12.5 mm) Nominal Maximum Aggregate Size (NMAS), was used in all lanes except for the top 2 inch (50 mm) layer of Lane 1, where gradation B and the CR-AZ asphalt rubber binder were used. The Los Angeles abrasion of the coarse aggregate was 19, and the sand equivalent was 75. All of the aggregates were from the Loudoun Quarry, Herndon, VA, except for the sand, which was from Luck Stone, Leesburg, VA. To reduce the potential for moisture damage, 1.0 percent hydrated lime was included in all mixes (*3*).

The gradation for the mix with fiber could be considered a third gradation. The only difference between its gradation and the other 0.5 inch (12.5 mm) NMAS gradation is that the fiber is considered part of the aggregate. Table 1 presents both gradations.

ALF Loading

The ALF machines are 95 feet (29 m) long frames with rails to direct rolling wheel loads. Each ALF machine is capable of applying an average of 35,000 wheel passes per week with a half-axle load. The applied load can range from 7500 to 19,000 lbf (33 to 84 kN). For fatigue tests, the load was applied uni-directionally at a loading speed of 11 mi/hr (18 km/hr) and load level of 16.6 kips (74 kN). Furthermore, the ALF machines were equipped with super-single (425/65R22.5 wide base) tires with tire pressure of 120 psi (0.83 MPa).

Table 1. Aggregate Gradations Used in the FHWA-ALF Tests (2).

Gradation Sieve Size		0.5 inch (12.5 mm) NMAS Superpave Mix			CR-AZ Mix	
(inch)	(mm)	Proposed by the Paving Contractor	Used by FHWA for Mix Design	Mix with 0.2 % Fiber	Aggregate	Crumb Tire Rubber
3/4	19.0	100.0	100.0	100	100.0	
1/2	12.5	93.0	93.6	93.6	87.0	
3/8	9.5	84.0	84.6	84.6	73.0	
No. 4	4.75	57.2	56.7	56.8	33.0	
No. 8	2.36	34.2	34.9	35.1	16.0	100.0
No. 16	1.18	22.5	24.8	25.0	11.0	98.3
No. 30	0.600	16.1	18.2	18.4	8.0	51.3
No. 50	0.300	11.6	13.1	13.3	6.0	11.9
No. 100	0.150	8.4	9.3	9.5	5.0	-
No. 200	0.075	6.3	6.7	6.9	3.0	0.6
Bulk dry SG		-	2.947	2.934	2.948	-
Bulk SSD SG		-	2.9365	2.952	2.971	-
Apparent SG		-	3.001	2.987	3.019	-
Water Abs., %		-	0.60	0.60	0.79	-

Note: SG – Specific gravity; SSD – Saturated surface dry; Abs. – Absorption.

FHWA-ALF FATIGUE TEST RESULTS

All the fatigue tests were conducted at a test temperature of 66.2 ºF (19 ºC). Up to now, six of the seven test lanes with 4 inch (100 mm) thick asphalt concrete (AC) pavements have been tested. The available fatigue cracking data (Lanes 1 to 6) are shown in Figure 2 (*3*). Lane 1 was excluded from the following analysis because two different asphalt mixes were used. In all other lanes, a single HMA mix was used. Thus, the following study (laboratory testing, FWD, and fatigue analyses) focused only on Lanes 2 to 6.

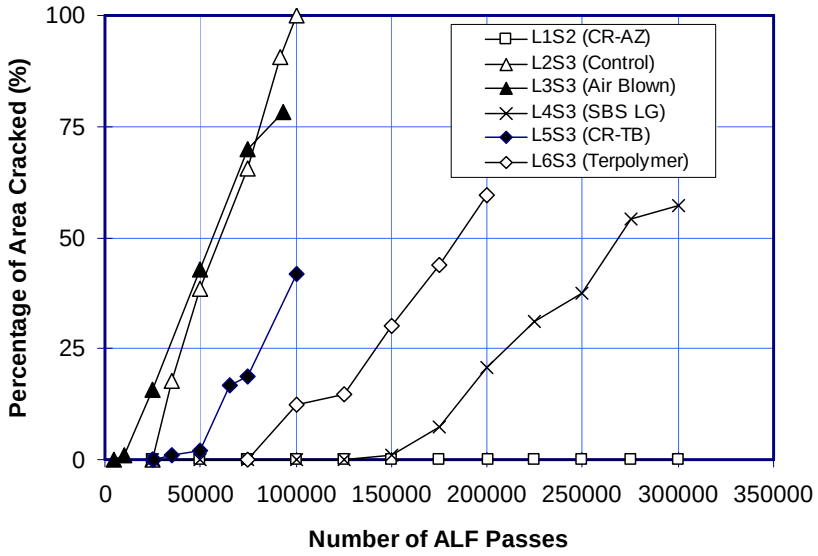

Figure 2. ALF Fatigue Test Results (*3*).

FWD TESTS AND BACKCALCULATED PAVEMENT LAYER MODULUS

FWD tests were conducted on top of the HMA surface layer shortly after the construction. Tests were conducted midway between the survey plates along the centerline of the each test site. Since eight survey plates were installed per site, a total of seven locations were tested. At each location, load levels of 6000, 9000, 12,000, and 16,000 lbs (2700, 4100, 5500, and 7300 kg) were used. Each load was dropped three times to measure its repeatability. This resulted in a total of 12 tests per location, 84 tests per test site, and 4032 tests for all 12 pavements. For all tests, nine sensors were used at distances of 0, 8, 12, 18, 24, 36, 48, 60, and -12 inches (0, 203, 229, 305, 457, 610, 914, 1219, 1524, and -229 mm) from the center of the load plate. The FWD tests were conducted in March and September 2003 under different pavement temperatures, respectively (*4*).

The MODULUS 6 software was used to backcalculate the modulus the pavement layers (*5*). Since it is well known that the moduli of granular base and subgrade are stress-dependent, the moduli of pavement layers, especially for granular base and subgrade, should be backcalculated at the FWD load level, which is same or similar to the ALF load level for fatigue test (16.6 kip [74 kN]). Therefore, the highest load level (16 kip [71.2 kN]) of FWD test was used to backcalculate the moduli of pavement layers. The detailed backcalculations for each test lane tested in March and September 2003 are presented in Appendices A and B, respectively. Table 2 lists the summary results.

Table 2. Backcalculated Pavement Layer Modulus.

Test Lanes	Modulus (ksi) @ Mar. 2003, $Temp_{pavement}$ = 43.5 ºF			Modulus (ksi) @ Sept. 2003, $Temp_{pavement}$ = 87.3 ºF		
	Asphalt Layer	Base	Subgrade	Asphalt Layer	Base	Subgrade
2	1853.2	8.4	7.6	761.2	9.3	6.3
3	1167.7	7.5	5.8	483.0	7.4	5.0
4	1570.8	8.0	6.7	482.7	8.2	5.4
5	910.1	6.5	5.2	440.4	6.4	4.6
6	1715.9	7.0	6.7	402.2	6.5	4.9

For granular base and subgrade, it is well known that they are not very sensitive to test temperature, which has been validated by the results presented in Table 2. Therefore, for base and subgrade layers, the average value of layer moduli in March and September 2003, as shown in Table 3, was used for later analyses.

Table 3. FHWA-ALF Pavement Layer Modulus for Analyses.

Test Lanes	$\lvert E^* \rvert$ of AC Layer (ksi)	Base Layer (ksi)	Subgrade (ksi)
2	813.9	8.8	6.9
3	742.8	7.5	5.4
4	578.1	8.1	6.0
5	536.7	6.5	4.9
6	498.4	6.8	5.8

LABORATORY DYNAMIC MODULUS TESTS OF HMA MIXES

In contrast to granular base and subgrade soil, HMA mixes are very sensitive to both loading time and testing temperature. Therefore, asphalt layer moduli backcalculated from FWD data were not applicable to analyze the ALF fatigue test, because the ALF operation speed was around 11 mi/hr (18 km/hr), and its corresponding loading time was much longer than that of FWD. Therefore, asphalt layer modulus for each lane was chosen based on dynamic modulus test results on field cores instead of FWD backcalculated modulus.

The dynamic modulus tests were conducted following the procedures described in the NCHRP 465 report (*6*). Figure 3 shows the test results at 66.6 ºF (19 ºC) (*7*). However, the

question was which frequency should be used for asphalt layer modulus of each lane for further analysis? Fortunately, the pavement responses under different load levels were measured using strain gauges during the shake-down testing (*4*). An example of the measured strain response at the bottom of asphalt layer is presented in Figure 4. It can be observed that the loading duration was approximately 0.2 second. Based on this information, a frequency of 5 Hz was used to determine the dynamic modulus of asphalt layer for each lane. The selected modulus for each lane is also presented in Table 3.

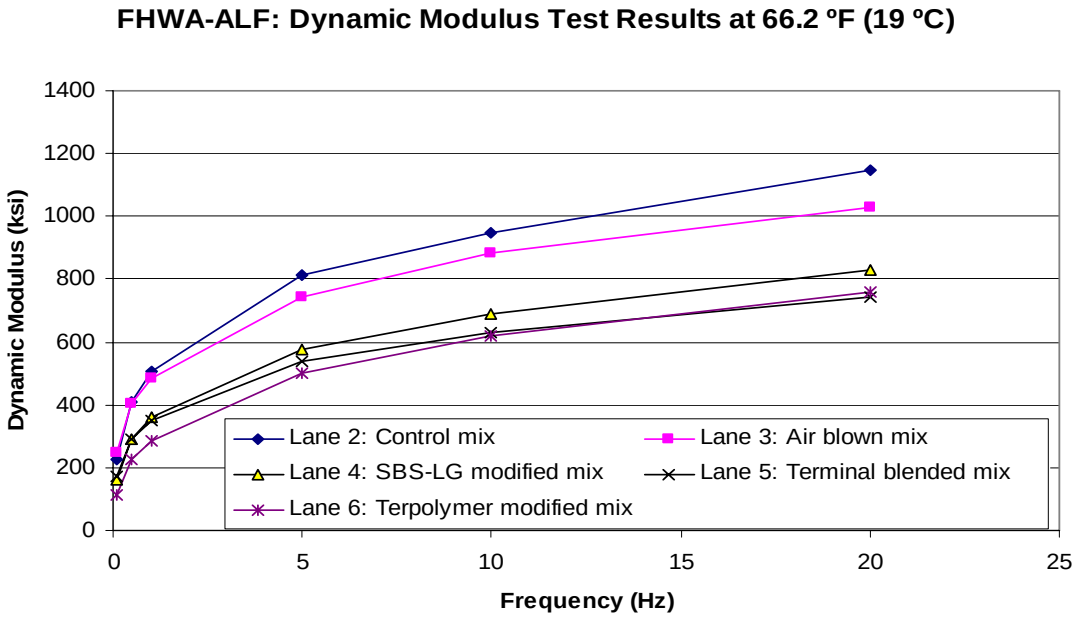

Figure 3. Dynamic Modulus Test Results for Each ALF Fatigue Test Lane (*7*).

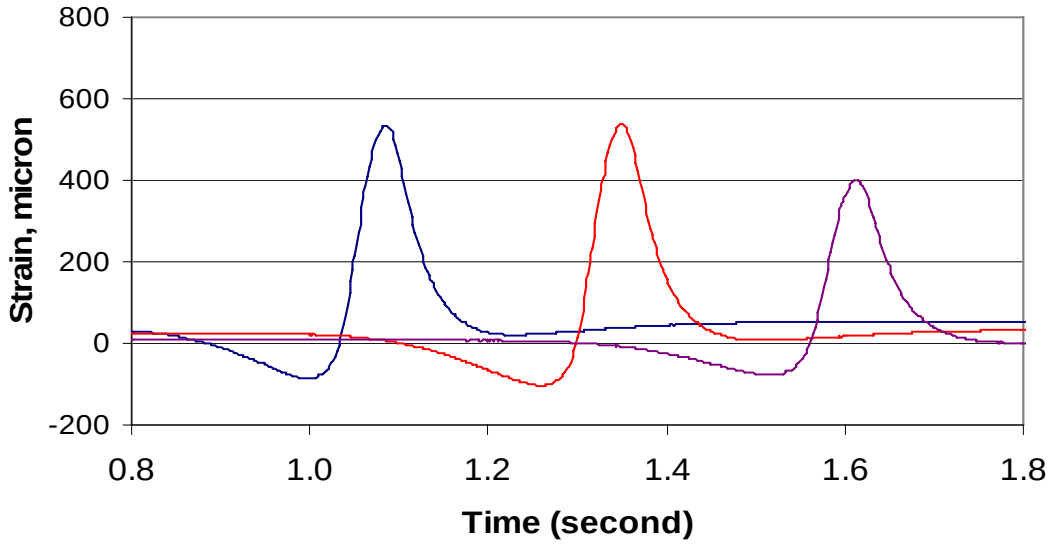

Figure 4. Typical Longitudinal Strain Response (*4*).

SUMMARY

This chapter described the FHWA-ALF fatigue test program and associated test results. In addition, FWD tests and laboratory dynamic modulus tests and associated results are also presented in this chapter. Specifically, this chapter discussed the approaches used to select pavement layer modulus for asphalt layer, granular base, and subgrade for further analyzing the FHWA-ALF fatigue test results.

CHAPTER 3

VERIFICATION OF THE MEPDG FATIGUE CRACKING MODEL

MEPDG FATIGUE CRACKING MODELS

The NCHRP 1-37A research team examined the Shell Oil and the MS-1 fatigue models for the MEPDG (*8*). It was found that the Shell Oil fatigue model possessed more scatter and did not possess any definite trends to follow; the MS-1 fatigue model had much less scatter and resulted in a definite trend. The MS-1 model was finally selected and implemented in the MEPDG. Different from the traditional fatigue cracking models, the MEPDG fatigue cracking model actually includes three models: fatigue life model, fatigue damage model, and fatigue cracking amount model. These three models are presented below.

- Fatigue life model

The number of the load repetitions predicted from fatigue life model (0.9 version) is below:

$$N_f = 0.007566 * k_1 * \left(\frac{1}{\varepsilon_t}\right)^{3.9492} \left(\frac{1}{E}\right)^{1.281} \quad (1)$$

where:

ε_t = tensile strain at the critical location,

E = stiffness of HMA mix (psi),

h_{ac} = asphalt layer thickness (inch),

k_1 = shift factor, defined below:

$$k_1 = \frac{1}{0.000398 + \frac{0.003602}{1 + e^{11.02 - 3.49 * h_{ac}}}} \quad (2)$$

For FHWA-ALF 4 inch (100 mm) thick fatigue test lanes, $k_1 = 262$.

- Fatigue damage model

The damage caused by different traffic loads is calculated as the ratio of the predicted number of load repetitions to the allowable number of load repetitions predicted by the fatigue life model, as shown in Equation 1.

$$D = \sum_{i=1}^{T} \frac{n_i}{N_i} \quad (3)$$

where:

D = fatigue damage,

T = total number of periods,

N = actual traffic for period i, and

N_i = allowable failure repetitions under conditions prevailing in period i.

- Fatigue cracking amount model

Finally, another transfer function to calculate the fatigue cracking amount was developed and calibrated using the long term pavement performance (LTPP) data. The final fatigue damage versus cracking amount model in the MEPDG is described as follows:

$$FC = \left(\frac{6000}{1 + e^{C_1 + C_2 * \log D}} \right) * \left(\frac{1}{60} \right) \quad (4)$$

where:

FC = percentage of fatigue cracking of total lane area,

D = damage (Equation 3), and

C_1, C_2 = calibration factors.

Note that Equation 4 is a sigmoidal function form, which is bounded with 0 percent cracking as a minimum and 100 percent cracking as a maximum. Specifically, it was assumed that a fatigue cracking value of 50 percent cracking of the total area of the lane theoretically occurs at a damage percentage of 100 percent. This assumption clearly indicates the following relationship:

$$C_1 = -2 \times C_2 \quad (5)$$

In the MEPDG, a_2 (Equation 16) is a function of asphalt layer thickness.

$$C_2 = -2.40874 - 39.748 \times \left(1 + h_{ac}\right)^{-2.85609} \quad (6)$$

where h_{ac} is the same as defined before. For the FHWA-ALF 4 inch (100 mm) fatigue test lanes, C_1= 5.6192 and C_2= -2.8096.

VERIFICATION OF THE MEPDG FATIGUE CRACKING MODELS USING FHWA-ALF DATA

As discussed in Chapter 2, all the FHWA-ALF fatigue tests were conducted at the same temperature: 66.2 ºF (19 ºC), and this temperature was kept constant during the testing. Thus, the only variable required for calculating for each lane is the tensile strain at the bottom of the

asphalt layer. Based on the experimental structural information and material properties presented in Chapter 2, the tensile strain at the bottom of asphalt layer for each lane was calculated by using a multi-layer elastic program, and the results are presented in Table 4. The fatigue life of each lane predicted from the MEPDG model (Equation 1) is also presented in Table 4. The fatigue cracking amount for Lanes 2 to 6 predicted from the MEPDG model (Equation 4) is plotted in Figures 5 to 9, respectively.

Reviewing Figures 5 to 9, it can be seen that the MEPDG fatigue cracking model underestimated fatigue cracking for Lanes 2 and 3 in which unmodified asphalt binders were used. On the other hand, the MEPDG fatigue cracking model overestimated the fatigue cracking in Lanes 4, 5, and 6 where modified asphalt binders were applied. Thus, for these five FHWA-ALF fatigue cases, the MEPDG fatigue cracking model, regardless of asphalt binder type (modified or unmodified), did not provide a reasonable prediction. This unsatisfactory prediction stimulates the development of the OT based fatigue cracking model. The detailed development is presented in the next chapter.

Table 4. Lanes 2 to 6: Fatigue Cracking Predictions.

ALF Test Lane	Lane 2	Lane 3	Lane 4	Lane 5	Lane 6
Tensile Strain, ε	5.458E-4	6.208E-4	7.097E-4	9.173E-4	8.324E-4
N_f before Shifting	1274	1037	858	343	480
N_f after Shifting	333,794	271,823	224,726	89,745	125,704

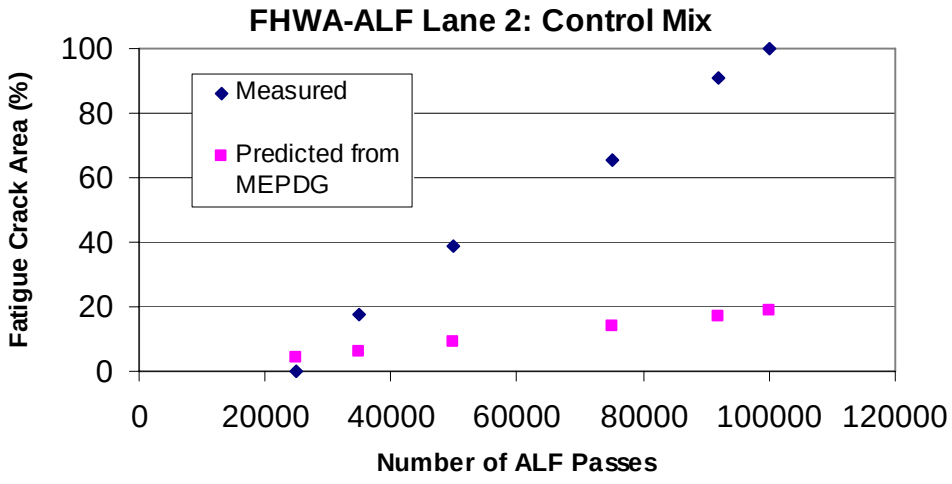

Figure 5. Lane 2: Fatigue Cracking Amount Predicted from the MEPDG Model.

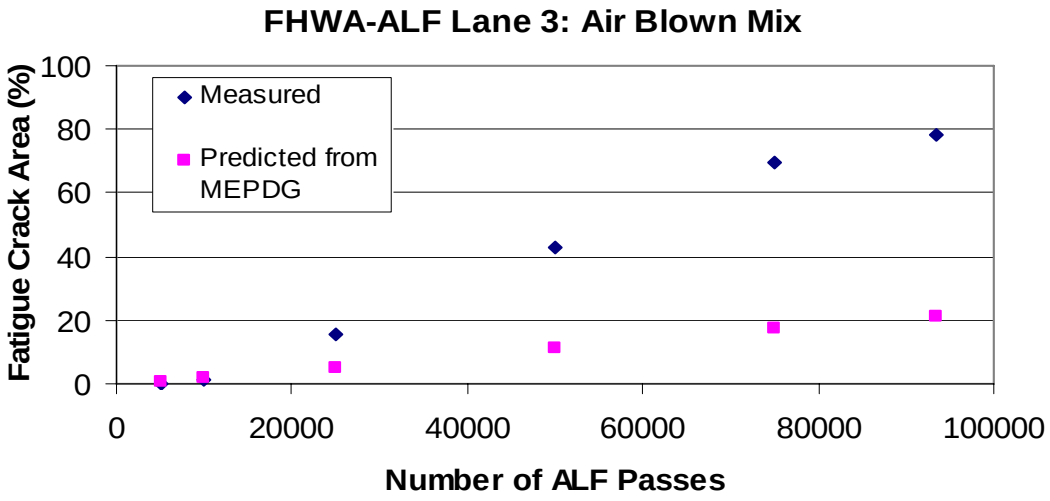

Figure 6. Lane 3: Fatigue Cracking Amount Predicted from the MEPDG Model.

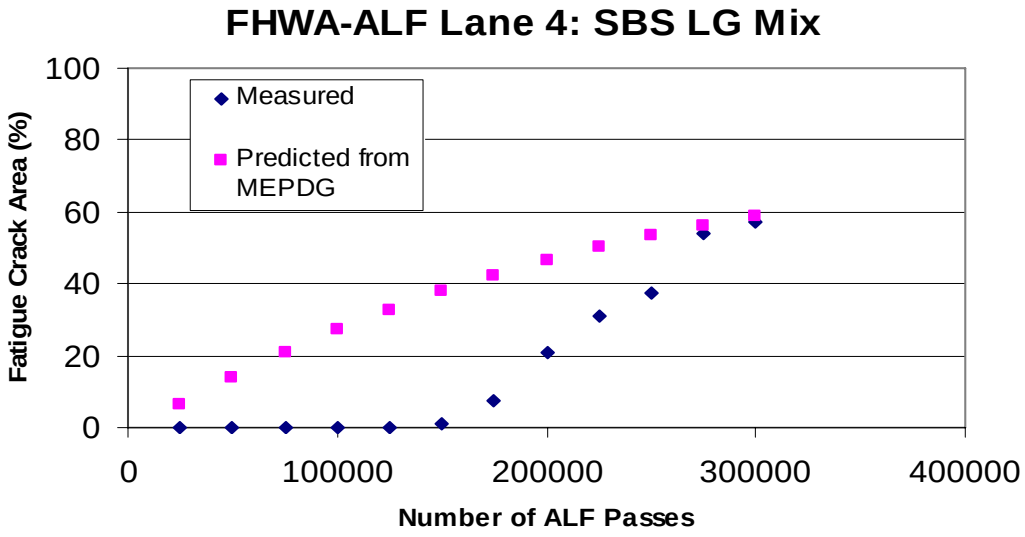

Figure 7. Lane 4: Fatigue Cracking Amount Predicted from the MEPDG Model.

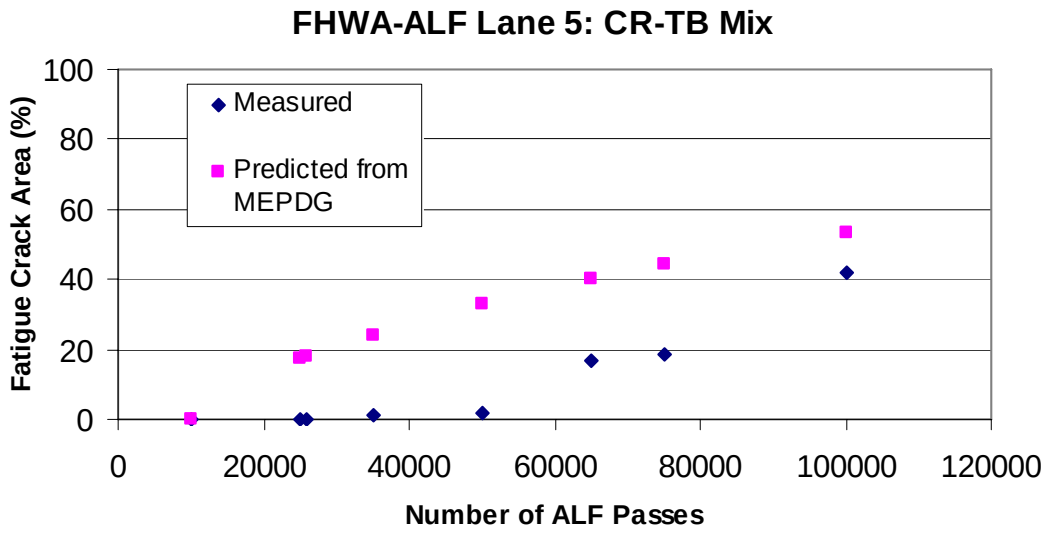

Figure 8. Lane 5: Fatigue Cracking Amount Predicted from the MEPDG Model.

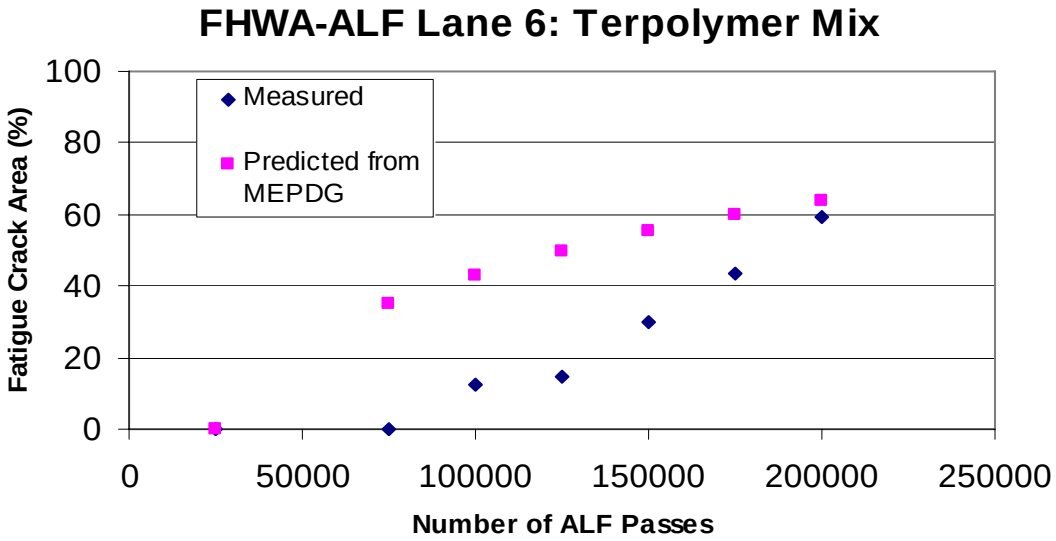

Figure 9. Lane 6: Fatigue Cracking Amount Predicted from the MEPDG Model.

SUMMARY AND FINDINGS

This chapter described the MEPDG fatigue cracking model, which is composed of the fatigue life model, fatigue damage model, and fatigue cracking amount model. To further verify these models, the FHWA-ALF fatigue test results were analyzed in this chapter. The fatigue cracking amount predicted from the MEPDG fatigue cracking model for each lane was compared with the measured. It was found that the MEPDG fatigue cracking model could not make a reasonable prediction for these five FHWA-ALF test lanes. Apparently, it is necessary to develop a more reasonable fatigue cracking prediction model which utilizes fundamental HMA mixture properties obtained from simple routine laboratory tests rather than time-consuming fatigue tests. Such an approach proposed in this project is discussed in the following chapter.

CHAPTER 4
DEVELOPMENT AND VERIFICATION OF THE OVERLAY TESTER BASED FATIGUE CRACKING PREDICTION APPROACH

INTRODUCTION

Generally, fatigue cracking starts from micro-cracks that grow and coalesce to form macro-cracks that finally penetrate through asphalt surface layer, which indicates that fatigue is a two-stage process: crack initiation and crack propagation. However, most of the traditional fatigue approaches including the MEPDG approach focused only on the crack initiation stage, and the crack propagation is considered through a large shift factor. As discussed in Chapter 3, the MEPDG approach could not accurately predict the fatigue performance of asphalt pavements. Therefore, comprehensive fatigue analysis approaches that take into account the complex nature of HMA mixes, pavement structure, traffic, environment, and other factors are needed to better predict fatigue performance of asphalt pavements. Fatigue cracking models associated with such approaches should have the potential to utilize fundamental HMA mix properties. Furthermore, it is desirable to obtain these fundamental material properties from simple routine laboratory tests rather than time-consuming fatigue tests. Such an approach called the OT based fatigue cracking prediction approach was proposed in this project.

This approach in which the OT is used to characterize fracture properties of HMA mixtures (A and n) was developed based on fracture mechanics. The fundamental HMA fracture properties (A and n) were used to estimate fatigue life of asphalt pavements. However, not only is the fatigue crack propagation considered, but the crack initiation (the number of load repetitions required to form a macro-crack from micro-cracks) is also included in this approach. Therefore, the approach presented is different from traditional fatigue crack approaches (such as the fatigue models used in the MEPDG) in which the fatigue crack propagation stage is not directly considered; it is also different from the often used fracture mechanics approaches in which the fatigue crack initiation stage is often ignored. The subsequent text presents the detailed work conducted in this project.

BACKGROUND OF THE OVERLAY TESTER

The first OT was designed by Germann and Lytton in the late 1970s (*9*). The key parts of the apparatus, as shown in Figure 10, consist of two steel plates, one fixed and the other which

moves horizontally to simulate the opening and closing of joints or cracks in the old pavements beneath the overlay. The OT specimen is glued to the two steel plates, with half of its length resting on each plate. Since its development, the OT has been widely used to evaluate the effectiveness of different geosynthetic materials to retard reflective cracking (*10, 11, 12, 13, 14, 15*). Recently, Zhou and Scullion upgraded the OT system and successfully used it to evaluate reflective cracking resistance of HMA mixes (*16*). One important modification was establishing a standard specimen size of 6 inch (150 mm) long by 3 inch (75 mm) wide by 1.5 inch (38 mm) high. This size of specimen can be easily cut from a sample prepared by the Superpave Gyratory Compactor (SGC) or from a field core. Figure 11 shows the OT specimen preparation sequence.

Generally, the OT is run in a controlled displacement mode (Figure 12) at a loading rate of one cycle per 10 sec with a fixed maximum opening displacement (MOD). The data automatically recorded during the test include load, displacement, and temperature. As reported by Zhou and Scullion, the OT test results were repeatable and also sensitive to test conditions and main component of HMA mixes (such as asphalt contents) (*16*).

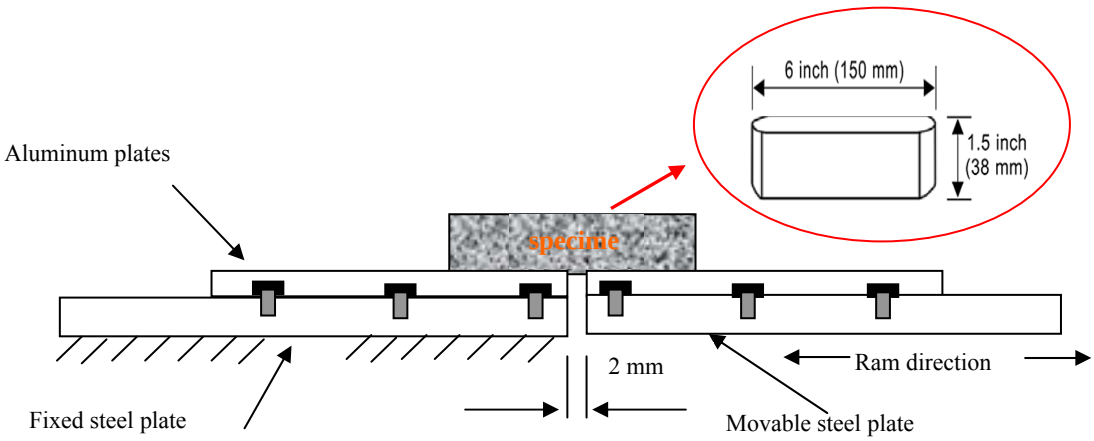

Figure 10. OT Concept.

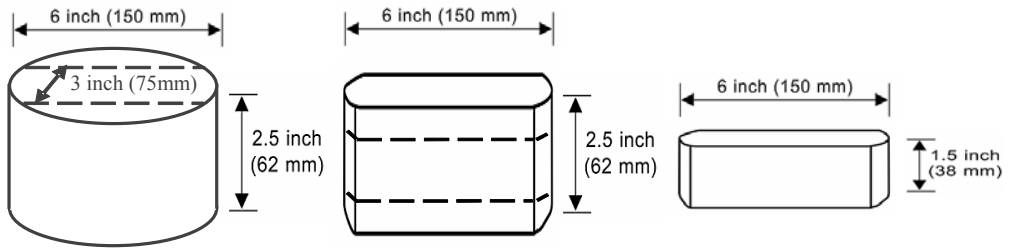

Figure 11. OT Specimen Preparation.

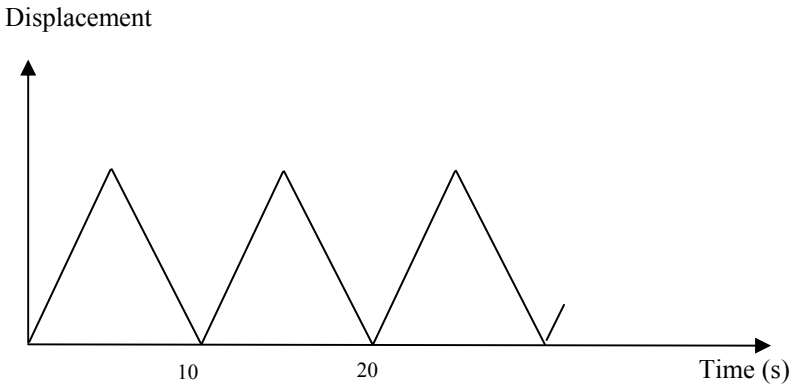

Figure 12. OT Loading Form.

With the above brief background information, how to determine fracture properties (*A* and *n*) of HMA mixes using the OT is presented below.

Determination of Fracture Properties: *A* and *n*

It is well known that HMA mixes are complex materials. However, for simplicity and practical applications, HMA mixes are often assumed to be quasi-elastic materials represented by dynamic modulus and Poisson's ratio. With this assumption, the well-known Paris' law shown in Equation 7 can be used to describe crack propagation of HMA mixes (*17*).

$$\frac{dc}{dN} = A(\Delta K)^n \qquad (7)$$

where:

c = crack length,

N = number of load repetitions,

dc/dN = crack speed or rate of crack growth,

ΔK = change of stress intensity factor (SIF), and

A, n = fracture properties of material.

In view of Equation 1, it can be seen that the information required for determining fracture properties (A and n) includes 1) the SIF corresponding to any specific crack length (c) and 2) crack length (c) corresponding to a specific number of load repetitions (N). The proposed approach for determining the SIF and crack length growth (c) is discussed as follows.

Determination of SIF

A 2-dimention finite element (FE) program named *2D-CrackPro* was developed under this project to analyze the SIF under the OT testing. In the *2D-CrackPro* program, the desired $1/\sqrt{r}$ stress singularity in the crack tip region was met by placing the mid-side nodes of two adjacent sides of an 8-node isoparametric element at one-fourth the distance from the common corner node (*18*). The accuracy of this program has been verified by comparing the computed SIFs of an infinite slab with a center crack with those given in "*the stress analysis of cracks handbook*" (*19*).

The 2-D FE mesh plus the singularity elements used are shown in Figure 13. Since Poisson's ratio has minor influence on SIF, a constant Poisson's ratio (υ=0.35) was used for all the analyses. With the above quasi-elastic assumption, it was found that the SIF is proportional to dynamic modulus (E) of the OT specimen and the specified MOD. Therefore, the SIFs corresponding to variable crack length (c) were calculated at an assumed condition: dynamic modulus of the OT specimen: E =1 MPa and MOD = 1 mm. The results are presented in Figure 14. To facilitate implementation, a regression equation shown in Figure 14 was developed for the SIF versus crack length at the condition of E=1 MPa and MOD = 1 mm.

For any other E and MOD combination, the corresponding SIF can be determined by the following equation:

$$SIF = 0.2911 * E * MOD * c^{-0.4590} \quad (8)$$

where:

SIF = stress intensity factor, MPa*mm$^{0.5}$,

E = dynamic modulus, MPa,

MOD = maximum opening displacement, mm, and

c = crack length, mm.

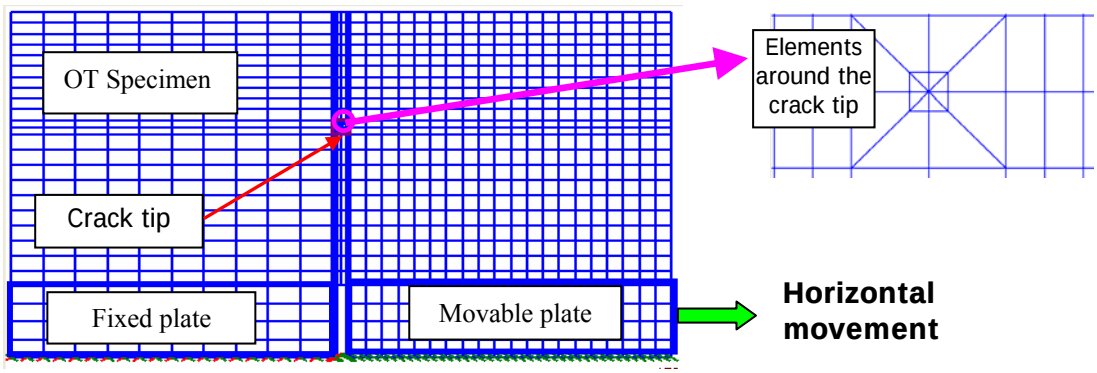

Figure 13. A 2-D FE Mesh of the OT System.

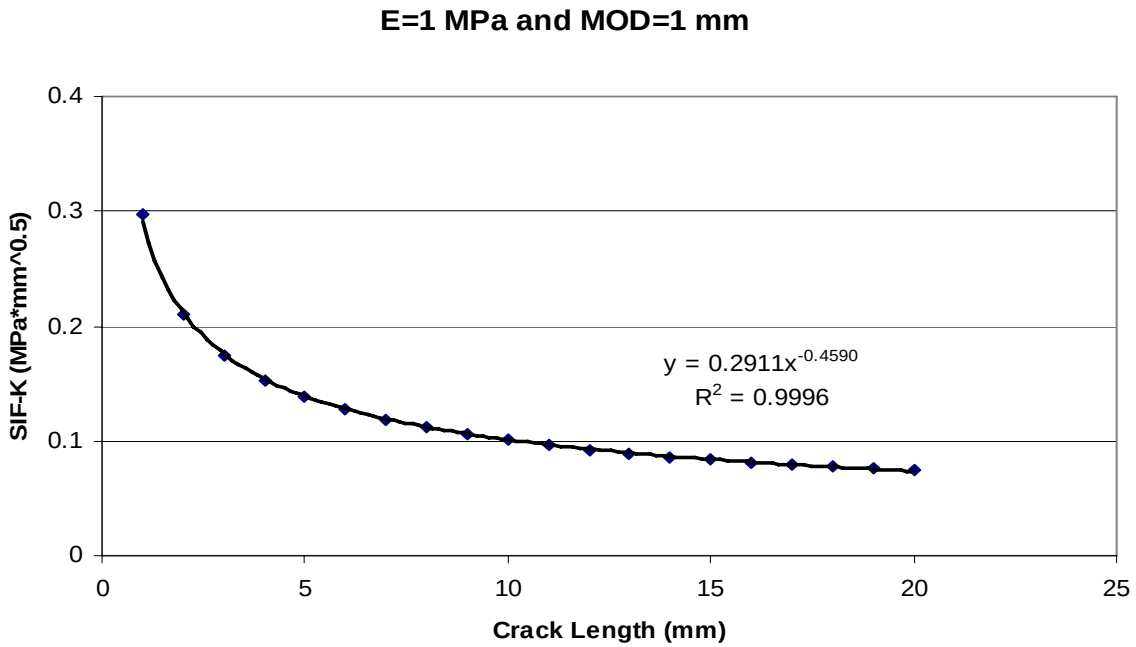

Figure 14. Calculated SIF vs. Crack Length.

Additionally, it can be seen that the SIF shown in Figure 14 decreases rapidly at the beginning, and its decreasing rate becomes smaller and smaller with crack length growth. This observation indicates that the initial crack propagation stage is very important to determine reasonable fracture properties of HMA mixes, which means that the required fracture properties can be determined from the initial stage of the OT testing (perhaps within 15 min.). This feature separates the OT from other types of fracture tests (such as, direct tension test [*20, 21, 22*],

indirect tension test [IDT] [*23*]), because the other tests often focus on the late crack propagation stage where the SIF increased rapidly so that these tests generally take a very long time (say, hours).

Determination of Crack Length (c)

To monitor crack length growth, researchers have used several different techniques such as crack foil (*21*). Recently, Seo et al. applied a Digital Image Correlation (DIC) technique to monitor crack propagation and crack length (*22*). The DIC is a non-contact, full-field displacement (or strain) measurement system that analyzes the displacement (or strain) by comparing digital images of deformed specimen with that of an initial undeformed specimen. Compared with other techniques, the DIC is one of most advanced techniques for crack propagation. However, application of the DIC system will definitely increase the difficulty and cost of running the OT. Fortunately, there is an alternative method used for estimating crack length; namely the backcalculation approach, which has been successfully used by Jacobs (*21*) and Roque et al. (*23*) to backcalculate the crack length from the recorded load or displacements. However, this backcalculation approach needs to be calibrated.

In this project, a calibrated backcalculation approach was proposed. Firstly, the crack length was backcalculated from the maximum load of each cycle measured in the OT based on theoretical analyses. Then, a DIC system with *two cameras*, as shown in Figure 15, was used to monitor crack growth. Finally, the backcalculated crack length was calibrated by comparing it with the measured crack length. However, at the time of writing this paper, the calibrating work is still underway; therefore, only the backcalculation part is presented below.

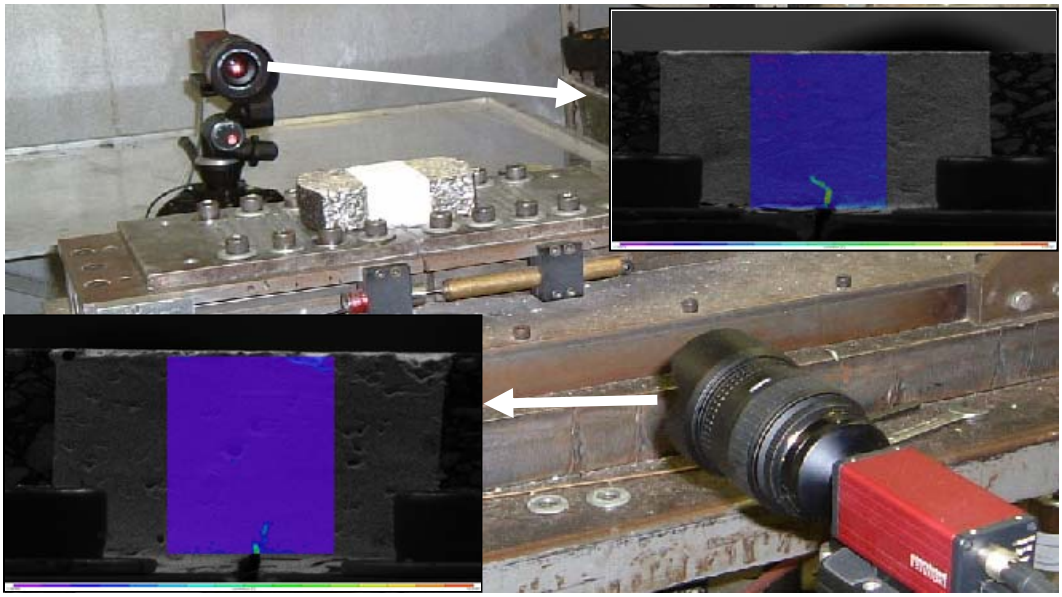

Figure 15. TTI's DIC System with the OT.

Researchers made three assumptions for establishing the theoretical relationship between equivalent crack length and maximum load required to reach a specified MOD:

- An equivalent (or ideal) crack starts from the bottom at the center of the OT specimen and propagates vertically to the top surface of the specimen.
- The reduction of maximum load from the first cycle is attributed to crack growth.
- As assumed previously, HMA mixes are quasi-elastic and represented by dynamic modulus and Poisson's ratio (υ=0.35).

With the above three assumptions, the maximum load required to reach a MOD is proportional to the dynamic modulus of the OT specimen and decreases with crack length growth, provided that the MOD is constant. To exclude the influence of the dynamic modulus and the MOD, the maximum load corresponding to any crack length was normalized to the maximum load corresponding to "zero" crack length, which is determined through extrapolation. Figure 16 shows the relationship between the normalized maximum load (y) and crack length (x). A corresponding regression equation is also presented in Figure 16.

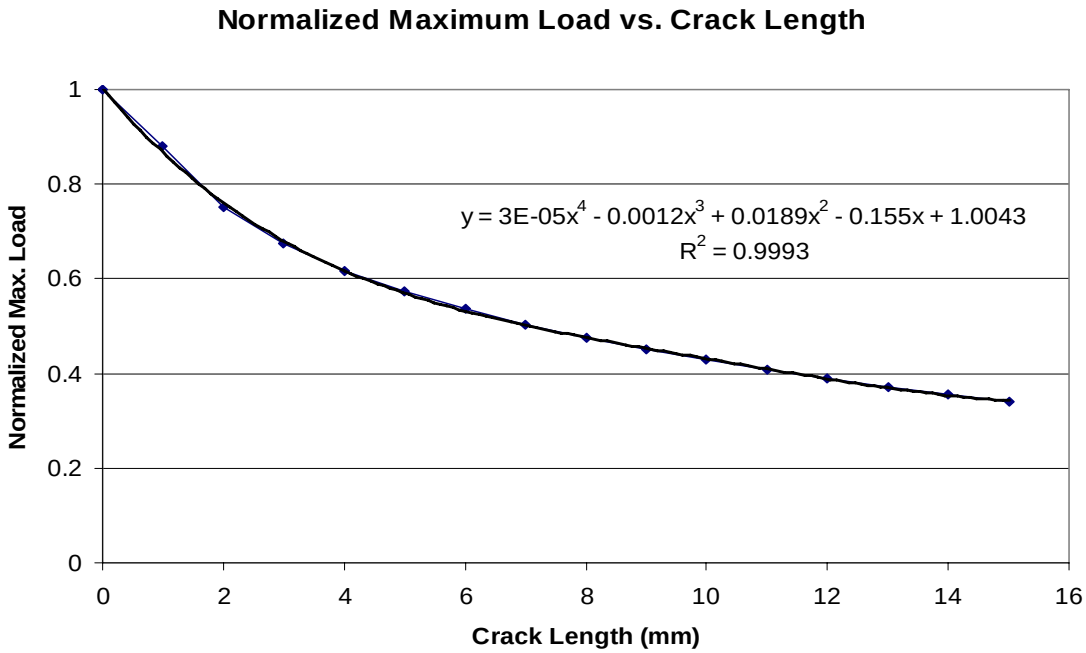

Figure 16. Normalized Maximum Load vs. Crack Length.

Since the maximum load at each cycle is automatically recorded during the OT testing, it is easy to develop the relationship between the normalized maximum load at each cycle and the number of cycles. Finally, combining with Figure 16, crack growth rate (d*c*/d*N*) can be calculated.

Determination of Fracture Properties: A and n

With known SIF (*K*) and crack growth rate (*dc/dN*), the fracture properties (*A* and *n*) can be readily determined. Figure 17 shows the five steps of determining fracture properties (*A* and *n*) of HMA mixtures. Currently, a Microsoft Excel® macro named *TTI-OT* is under development to automatically analyze the OT test results and determine fracture properties (*A* and *n*).

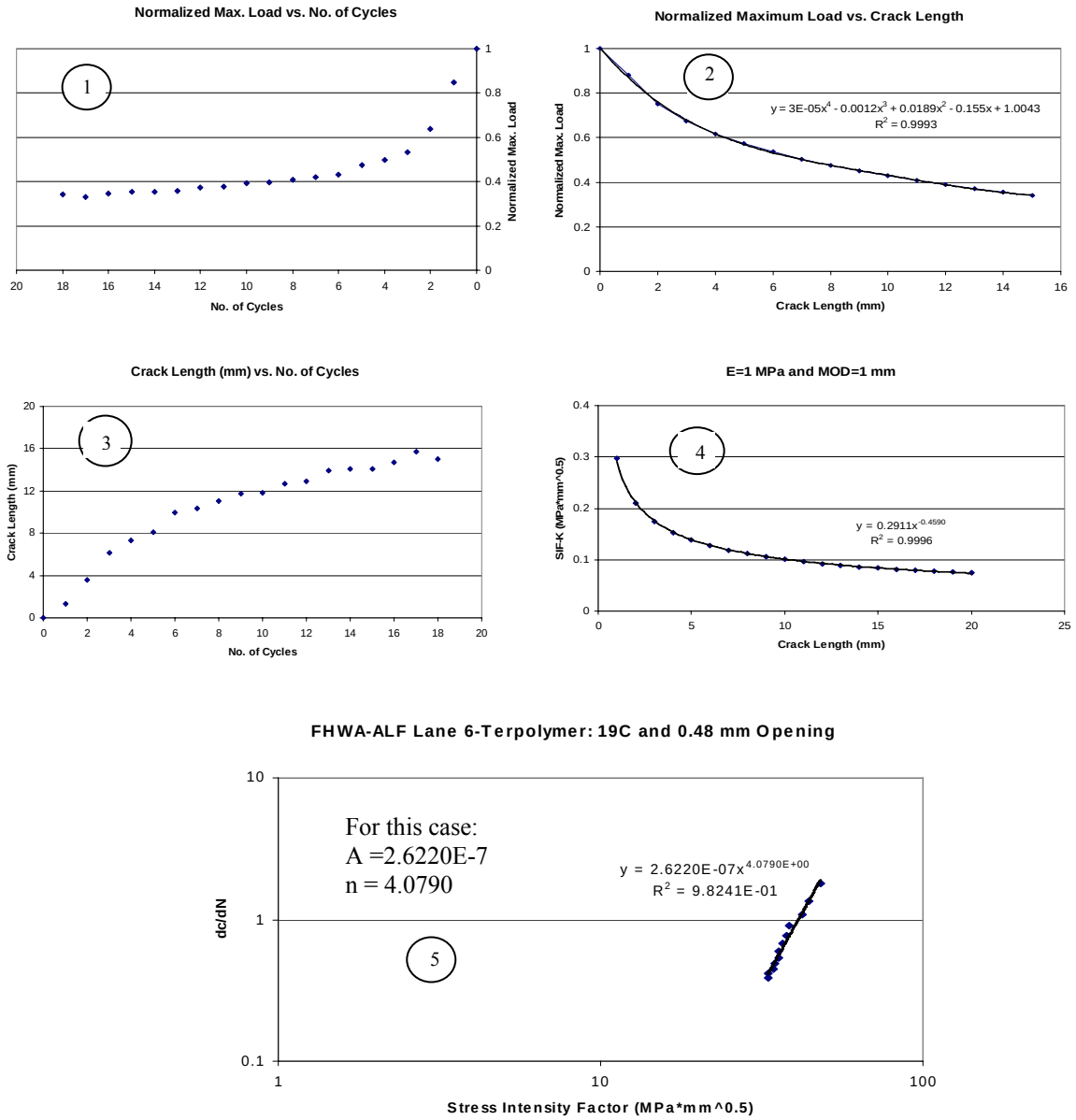

Figure 17. Determination of Fracture Properties: *A* and *n*.

In summary, the section focused on developing the methodology of determining fracture properties (*A* and *n*) using the OT. As listed below, this OT based methodology for fracture properties has several features:

- Specimen size (6 inch [150 mm] long by 3 inch [75 mm] wide by 1.5 inch [38 mm] high): This size of specimen can be easily cut from samples compacted by the SGC or from field cores.

- Specimen preparation (Figure 11): Neither a hole in the center nor a notch at the bottom of the specimen is required, since a crack is always initiated in the first cycle.
- Testing time: In contrast to other fracture types of tests (i.e. IDT or repeated direct tension test) which generally take a long time to run, the OT for fracture properties (A and n) can generally be done within 15 minutes.

Built on the foundation of determining the fracture properties of HMA mixes using the OT discussed above, a new fatigue crack prediction approach is proposed in the subsequent text.

THE OT BASED FATIGUE CRACKING PREDICTION APPROACH

As noted previously, fatigue cracking is the combination of crack initiation and crack propagation process. The number of traffic load repetitions (N_f) to cause a crack to initiate and propagate through the asphalt surface layer is the sum of the number of load repetitions needed for micro-cracks to coalesce to initiate a macro-crack (crack initiation, N_i) and the number of load repetitions required for the macro-crack to propagate to the surface (crack propagation, N_p).

$$N_f = N_i + N_p \tag{9}$$

In the OT based approach, both N_i and N_p are estimated from the fracture properties (A and n), which are determined from the OT. The detailed information is described as follows.

Estimation of N_i

It is well known that the traditional fatigue model established based on bending beam fatigue tests mainly addresses the crack initiation stage. Thus, in this project, the traditional fatigue model shown in Equation 10 is used to estimate N_i.

$$N_i = k_1\left(\frac{1}{\varepsilon}\right)^{k_2} \tag{10}$$

The key issue is to establish a "bridge" between fracture properties (A and n) and parameters k_1 and k_2. Based on fracture mechanics, Lytton et al. found the following relationships between these parameters (*24*). The detailed derivation about the relationship is presented in Appendix C.

$$k_1 = \frac{d^{\left(1-\frac{n}{2}\right)}}{Ar^n(1-nq)E^n}\left[1-\left(\frac{c_0}{d}\right)^{(1-nq)}\right] \tag{11}$$

$$k_2 = n \quad (12)$$

Equation 11 indicates that parameter k_1 (or $\log k_1$) is a function of k_2, A, and E:

$$\log k_1 = f(k_2, E, A) \quad (13)$$

As reported by Schapery (*25*), Molenaar (*20*), Jacobs (*21*), Lytton et al. (*24*), and Erkens et al. (*26*), the fracture property A is highly related to parameters n (= k_2) and $\log E$. Thus, it is reasonable to simplify Equation 11 as following form:

$$\log k_1 = a_1 + a_2 k_2 + a_3 \log E \quad (14)$$

where, a_1, a_2, and a_3 are regression constants. It is worth noting that a very similar relationship shown in Equation 14 can also been developed based on continuum damage mechanics (*27*). Detailed derivation from continuum damage mechanics is provided in Appendix D. Therefore, Equation 14 is theoretically sound. The key to estimating parameter k_1 becomes determining regression constants a_1, a_2, and a_3.

In order to do so, the results from historical fatigue test data were reviewed. It was found that the Bending Beam Fatigue Test (BBFT) is the most often used method to characterize fatigue behavior of HMA mixes. In this project, the researchers team assembled several sources of BBFT data and developed the required regression parameters in Equation 14. After carefully reviewing the available BBFT data, the following data sets were selected for modeling:

- SHRP A-003A fatigue data (*28*): 218 tests;
- Harvey et al. – 1996 (*29*): 211 tests;
- Sousa, et al. – 1998 (*30*): 129 tests;
- Tsai – 2002 – WesTrack fatigue data (*31*): 150 tests;
- Ghuzlan and Carpenter – 2003 (*32*): 478 tests; and
- Tsai et al. – 2005 (*33*): 162 tests.

The total number of available BBFT data sets was 1348. The test variables covered in these 1348 sets of data include type of asphalt binder (unmodified and modified), asphalt contents, type of aggregates, type of HMA mixes (dense-graded, Superpave, and SMA), air void contents, test temperatures, and aging conditions.

Using "Solver" optimization technique in Excel by minimizing the sum of squared errors between the measured and the predicted k_1, the regression constants a_1, a_2, and a_3 were determined, and the final k_1 equation is presented below. Figure 15 shows the predicted and the measured $\log k_1$.

$$k_1 = 10^{6.97001 - 3.20145 k_2 - 0.83661 \log E} \quad R^2 = 0.99 \qquad (15)$$

With the above Equations 10, 12, and 15, N_i can be estimated provided that tensile strain at the bottom of the asphalt layer and modulus of asphalt layer are known.

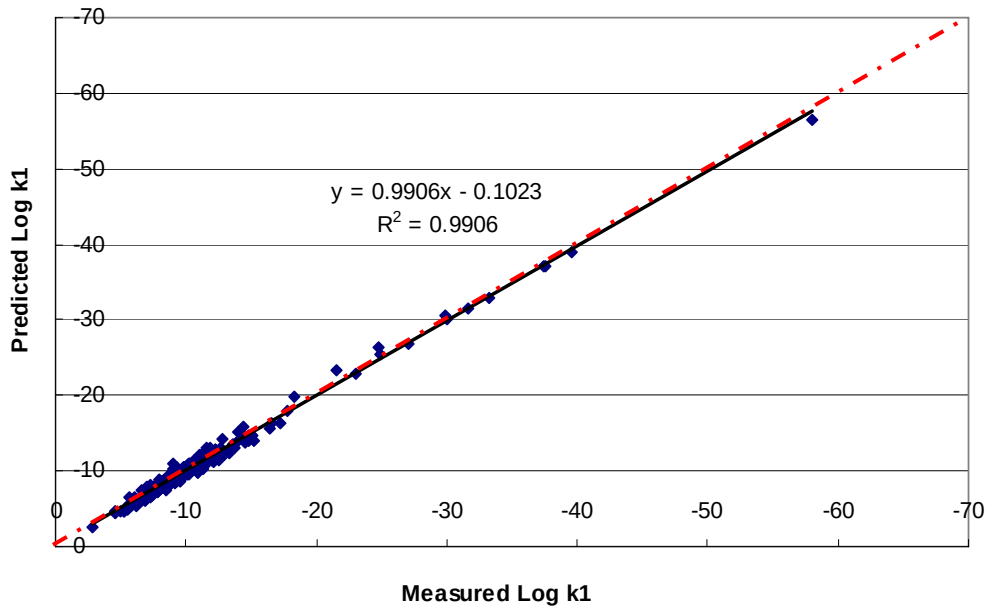

Figure 18. Predicted logk_1 vs. Measured logk_1.

Estimation of N_p

Theoretically, with known fracture properties A and n (from the OT) and SIF (from FE program), N_p can be estimated from Equation 10:

$$N_p = \int_{c_0}^{h} \frac{1}{A(\Delta K)^n} dc \qquad (16)$$

where, c_0 is the initial crack length and h is asphalt layer thickness. Based on micro-mechanics theory and laboratory test results, Lytton et al. recommended the initial macro-crack length (c_0) is equal to 0.3 inch (7.5 mm), which results from micro-crack growth *(24)*.

However, it is well known that one axle passing over a crack results in three loading sequences: shearing (approaching to a crack), bending (loading on the top of the crack), and shearing (leaving from the crack). These three loading sequences make it difficult to directly estimate N_p from Equation 10. In this project, an alternative approach was proposed.

Instead of estimating N_p from Equation 10, the authors recommended to calculate the crack propagation length induced by one axle pass using the following form of Paris' law:

$$\Delta c = A(\Delta K)^n \times \Delta N \quad (17)$$

Note that for one axle pass, a crack should propagate three times: Δc_s, Δc_b, and Δc_s, corresponding to the shearing, bending, and shearing loading sequence, respectively. Thus, the crack propagation length (Δc) induced by one axle pass is the sum of Δc_s, Δc_b, and Δc_s.

$$\Delta c = 2 \times \Delta c_s + \Delta c_b = A \times \left[2 \times \left(\Delta K_{Shearing}\right)^n + \left(\Delta K_{Bending}\right)^n\right] \times \Delta N \quad (18)$$

Add more axle passes, and repeat the above process until the accumulated crack length is equal to asphalt layer thickness (h). Then, N_p is the sum of all the number of passes.

The OT Based Fatigue Cracking Prediction Approach

Based on the information presented above, the OT based fatigue cracking prediction approach is proposed. The key steps of this OT based approach is summarized and presented below.

1. Run dynamic modulus test to develop dynamic modulus master curve of HMA mixtures.
2. Run the OT to determine fracture properties A and n of HMA mixes.
3. Estimate traditional fatigue model parameters k_1, k_2, and N_i from Equations 10, 12, and 15.
4. Compute the SIF caused by traffic load using FE programs.
5. Estimate N_p with an initial macro-crack length (c_0) using Equation 18.
6. Calculate N_f from Equation 9.
7. Calculate the damage caused by a specified number of load repetitions (n) using Miner's law (Equation 19).

$$\text{Damage} = \sum \frac{n}{N_f} * 100\% \quad (19)$$

8. Predict fatigue crack amount using the model proposed in the MEPDG (*1*).

$$\text{crack area}(\%) = \frac{100}{1 + \exp(a_1 + a_2 * \log \text{Damage})} \quad (20)$$

where:

a_1, a_2 = calibration coefficients:

$$a_1 = -2 \times a_2 \quad (21)$$

$$a_2 = -2.40874 - 39.748 \times (1 + h_{ac})^{-2.85609} \quad (22)$$

where:

h_{ac} = asphalt layer thickness (inch)

However, as shown later, a_2 needs to be recalibrated in order to make a reasonable prediction.

In summary, based on theoretical review and 1348 datasets of BBFT, a "bridge" (equations) between crack initiation model (traditional fatigue model) and crack propagation model (Paris' law) was developed in this section. An OT based fatigue cracking prediction approach including both crack initiation and crack propagation was then proposed. With the purpose of verification and demonstration, this proposed approach was used to analyze five FHWA's ALF fatigue tests with controlled loading and temperature as described below.

VERIFICATION AND DEMONSTRATION OF THE OT BASED FATIGUE CRACKING PREDICTION APPROACH

The FHWA-ALF fatigue test sections were selected for this verification and demonstration, since all necessary information was available. The detailed information is presented as follows.

Step 1: Run Dynamic Modulus Test on FHWA-ALF HMA Mixtures

As noted previously, the dynamic modulus tests have been separately conducted on field cores from these test lanes by Al-Khateeb et al. (*7*). Thus, in this project the dynamic modulus test was skipped, and the measured dynamic modulus for each lane from the reference *7* was directly used in the following analyses.

Step 2: OT Testing on Field Cores from FHWA-ALF Test Site

Field cores from the FHWA-ALF fatigue test lanes were taken and shipped to TTI for OT testing. The OT was run at 66.6 ºF (19 ºC) to match the FHWA-ALF testing temperature. As shown in Figure 12, the loading and unloading time for each cycle is 10 seconds in the OT. Thus, for specimens from each lane, the dynamic modulus corresponding to 0.1 Hz (≅1/10 s OT loading and unloading time), as shown in Table 5, was selected for calculating the SIF and determining fracture properties A and n.

Following the methodology for determining fracture properties using the OT (Figure 17), the fracture properties of each mixture were determined. Figures 19 to 23 show the results.

Table 5. Dynamic Modulus for Determining *A* and *n* *(7)*.

ALF Test Lane	Lane 2	Lane 3	Lane 4	Lane 5	Lane 6
|E*| @0.1Hz (MPa)	1553	1709	1096	1202	795

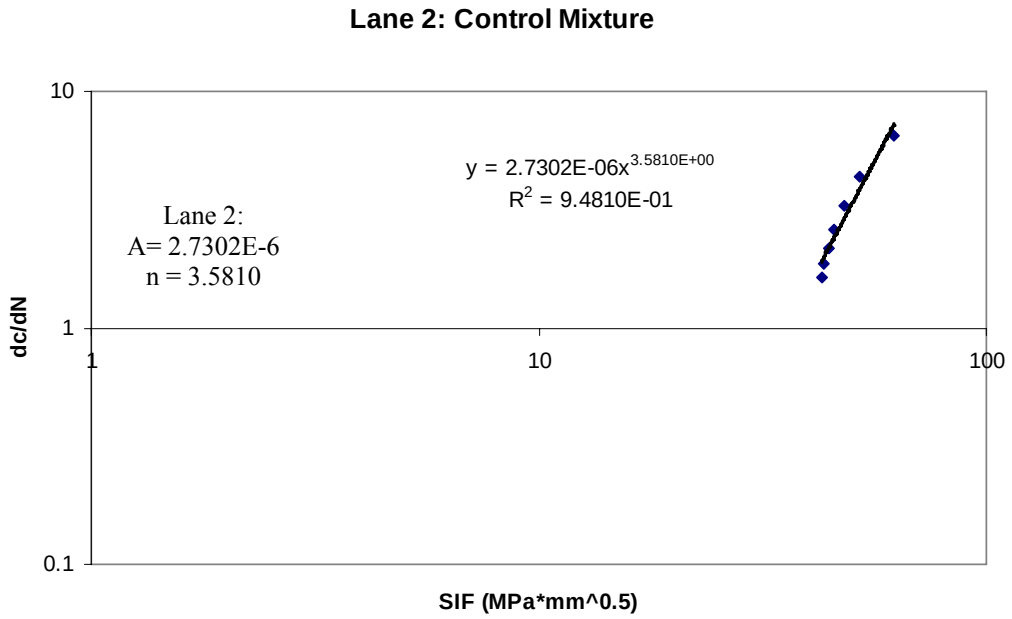

Figure 19. Lane 2: Fracture Properties: *A* and *n*.

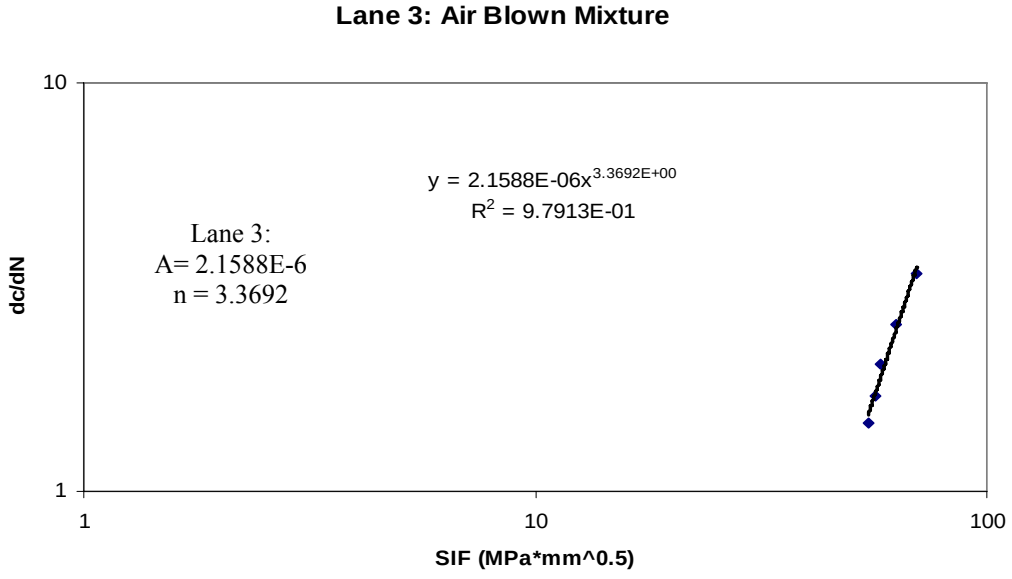

Figure 20. Lane 3: Fracture Properties: *A* and *n*.

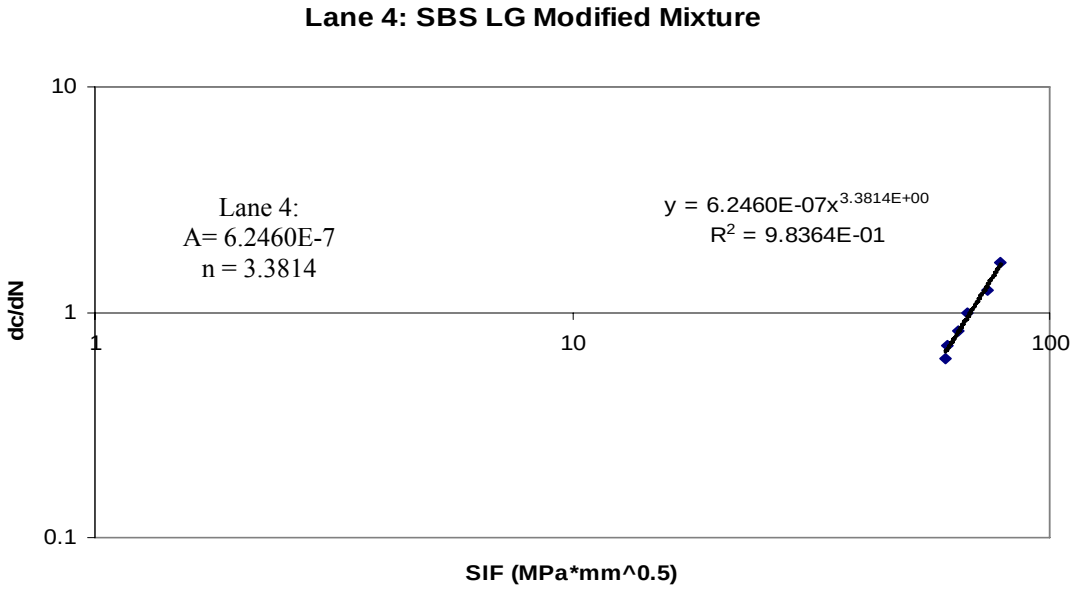

Figure 21. Lane 4: Fracture Properties: *A* and *n*.

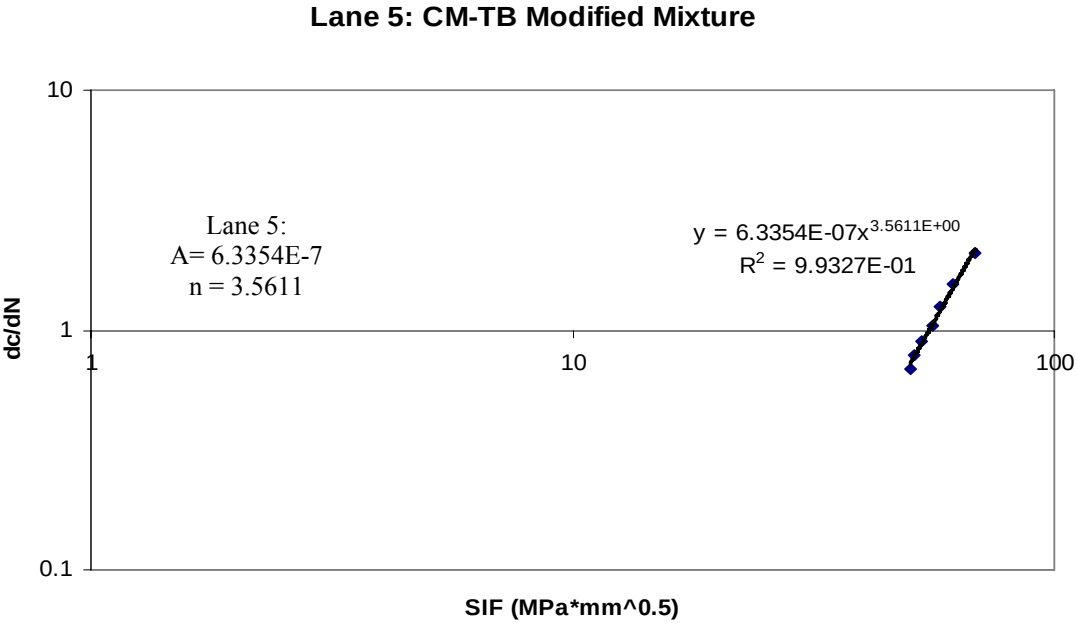

Figure 22. Lane 5: Fracture Properties: *A* and *n*.

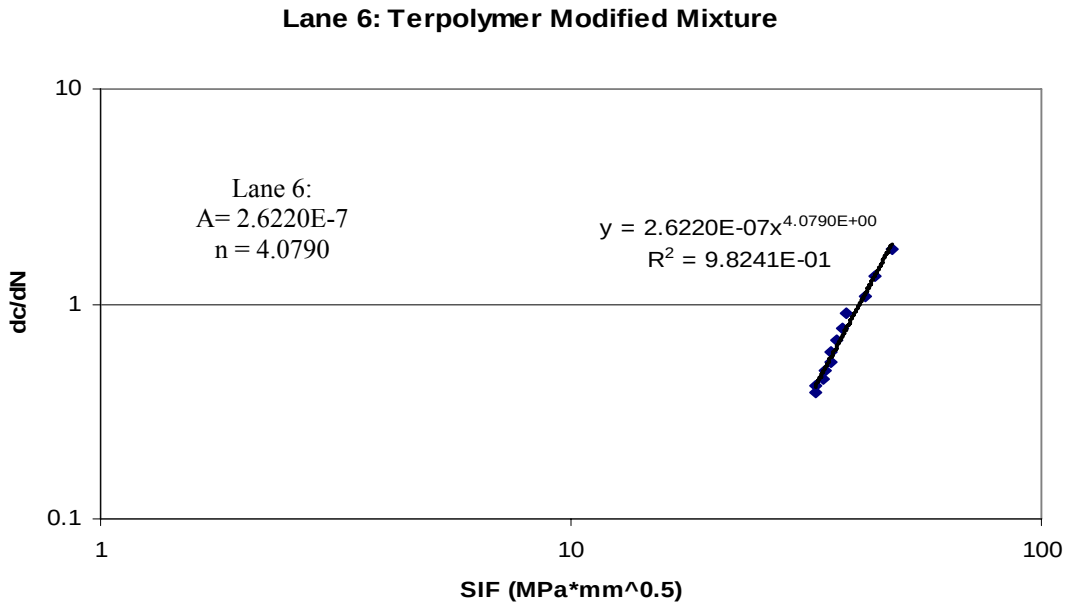

Figure 23. Lane 6: Fracture Properties: *A* and *n*.

Step 3: Estimate k_1, k_2, and N_i

In view of Equations 10, 12, and 15, it can be seen that the information needed to estimate k_1, k_2, and N_i includes 1) pavement structural thickness, 2) pavement layer modulus, and 3) ALF load level. Pavement structural and ALF load information has been described previously. Thus, only the determination of pavement layer modulus is discussed below:

Calculation of Tensile Strains and Estimations of k_1, k_2 and N_i

With the above known information, the tensile strains at the bottom of asphalt layer were computed using multilayer linear elastic program. k_1, k_2, and N_i for each asphalt layer was then estimated based on Equations 10, 12, and 15. Table 6 presents the calculated results.

Table 6. Lanes 2 to 6: Fatigue Cracking Predictions.

ALF Test Lane	Lane 2	Lane 3	Lane 4	Lane 5	Lane 6
A	2.7302E-6	2.159E-6	6.246E-7	4.561E-7	2.622E-7
N	3.5810	3.3692	3.3814	3.6410	4.0790
k_1	2.049E-8	1.190E-7	1.357E-7	2.131E-8	8.186E-10
k_2	3.5810	3.3692	3.3814	3.6410	4.0790
Tensile strain, ε	5.458E-4	6.208E-4	7.097E-4	9.173E-4	8.324E-4
N_i	9916	7601	6030	2444	2986
N_p	25,029	41,647	194,580	120,329	131,678
Predicted N_f (=N_i + N_p)	34,945	49,248	200,610	122,773	134,664
Measured N_f corresponding To 50% fatigue cracking area	59,025	56,548	270,000	118,000	189,329
Measured/predicted N_f	1.7	1.2	1.3	1.0	1.4

Step 4: Compute the SIF Caused by ALF Loading

Although 2-D FE programs run much faster than the three dimensional (3-D) FE programs, it is common knowledge that the SIFs computed from plane strain conditions are over estimated because of the difference between plane strain conditions and the 3-D nature of a cracked geometry and loading conditions. In order to balance the accuracy of 3-D FE (3-D nature of the cracked pavement geometry and the loading condition) and fast running time of 2-D FE, a semi-analytical FE program named *SA-CrackPro* was developed. This *SA-CrackPro* provides for adequate accuracy and efficient analysis of crack propagation in an asphalt layer with adequate accuracy. Similar to the *2-D CrackPro* program, singular elements were used in the *SA-CrackPro* program to model the stress singularity at the tip of the crack (*18*).

As noted previously, one ALF load pass induced bending and shearing stresses and associated bending SIF-$\Delta K_{bending}$ (loading on top of a crack) and shearing SIF- $\Delta K_{shearing}$ (loading at either side of the crack). With the known information of pavement structural thickness, layer modulus, and Poisson's ratio for the ALF lanes, *SA-CrackPro* program was used to compute bending and shearing SIFs for each test lane. Figures 24 to 28 present the computed bending and shearing SIFs for Lanes 2 to 6, respectively.

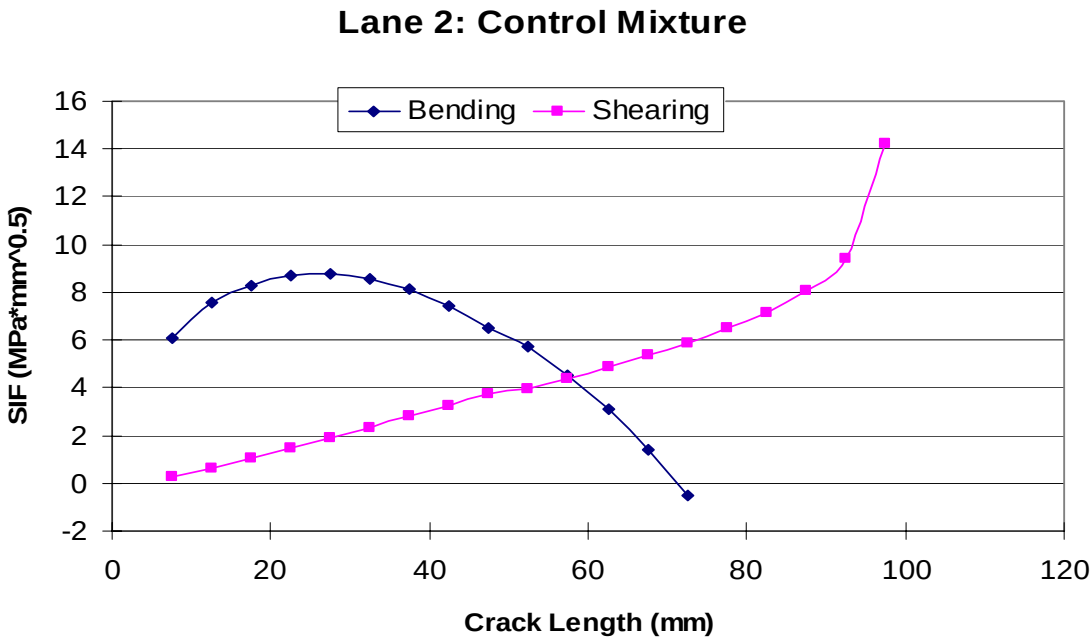

Figure 24. Lane 2: Computed Bending and Shearing SIFs.

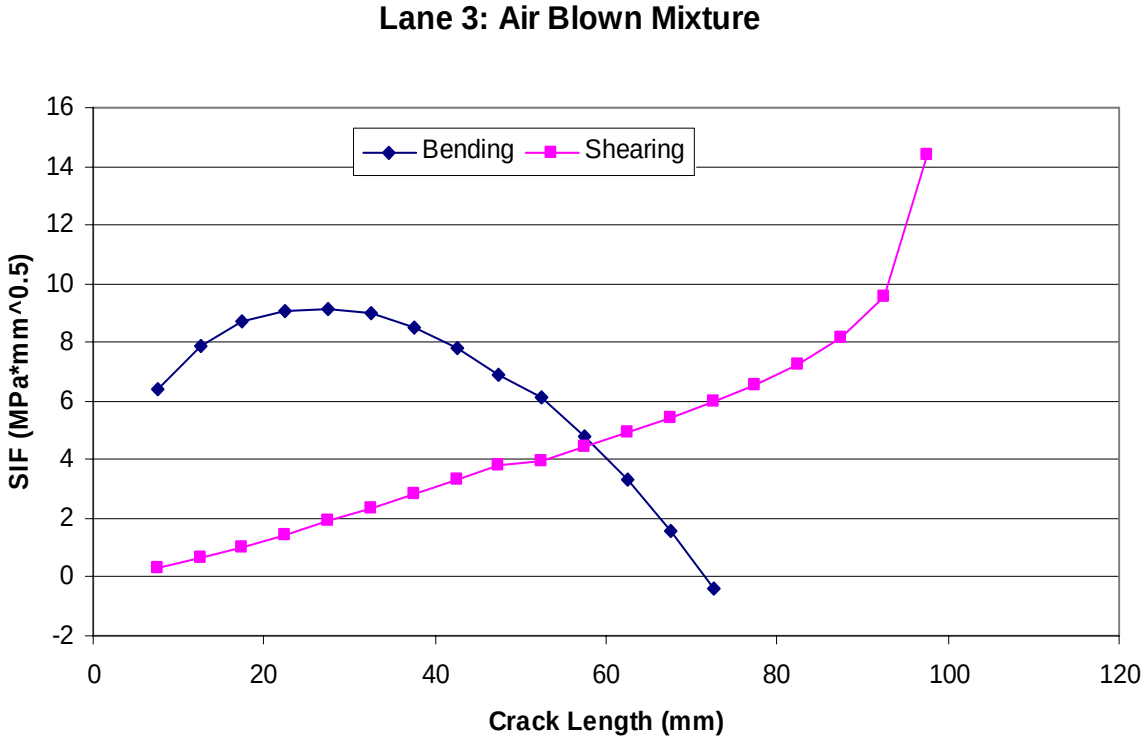

Figure 25. Lane 3: Computed Bending and Shearing SIFs.

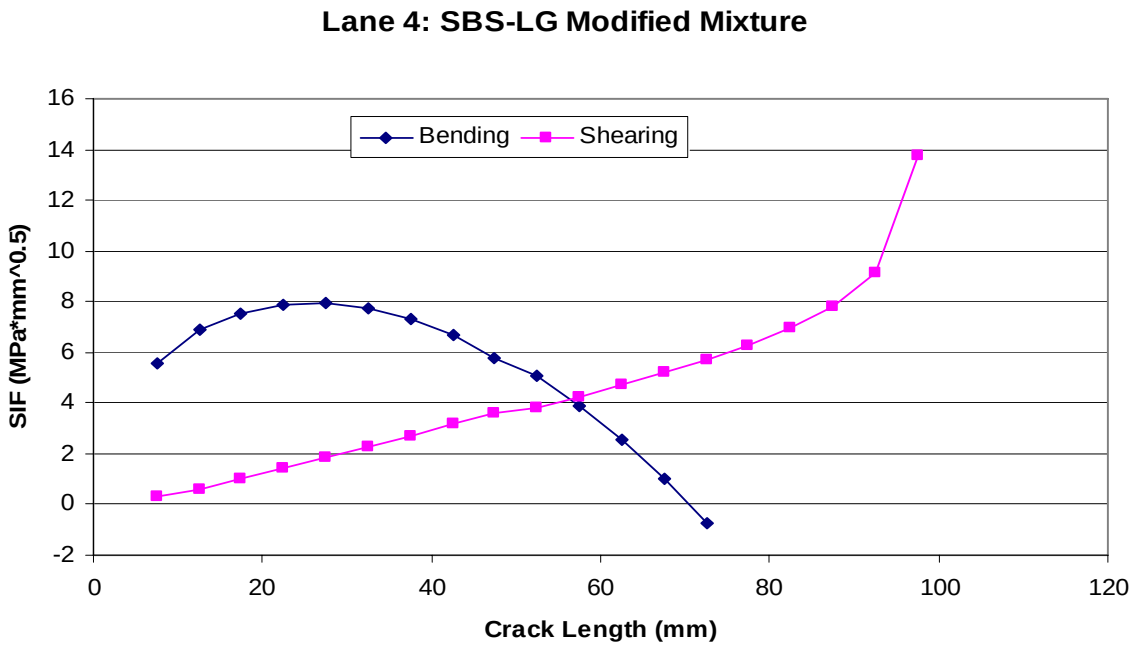

Figure 26. Lane 4: Computed Bending and Shearing SIFs.

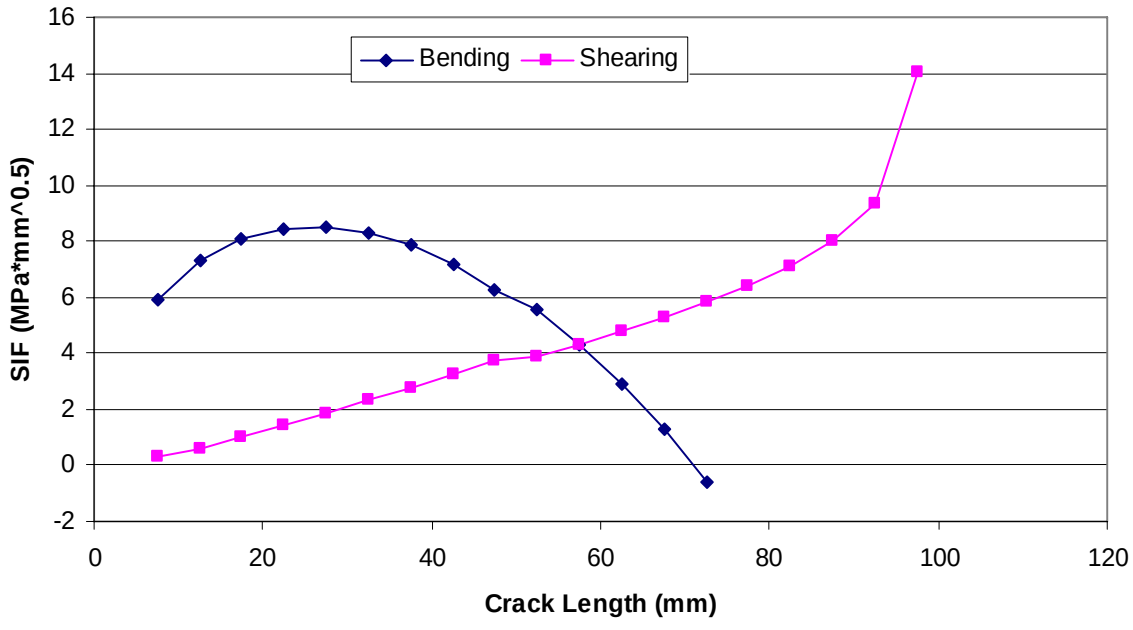

Figure 27. Lane 5: Computed Bending and Shearing SIFs.

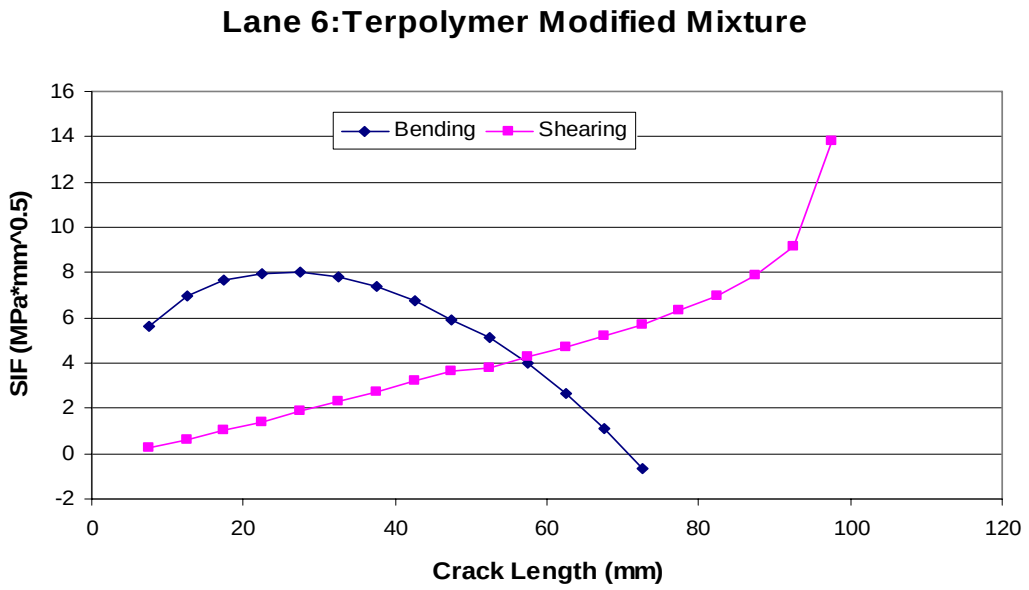

Figure 28. Lane 6: Computed Bending and Shearing SIFs.

Step 5: Estimate of N_p

As noted previously, one ALF load pass results in three crack propagations: Δc_s, Δc_b, and Δc_s. Following the approach described previously (Equation 18), N_p for each test lane was calculated. Table 6 presents the results.

Step 6: Calculate of N_f

The estimated fatigue life (N_f) for each test lane is the sum of the computed N_i and N_p. The results are also presented in Table 6.

In addition, the fatigue life for each test lane under ALF loading was also determined based on 50 percent cracking of the testing area, and each is listed in Table 6. Comparing the predicted with the measured fatigue life, a shift factor (the measured N_f/the calculated N_f) was developed for each test lane. As seen in Table 6, for all five cases, the averaged shift factor is 1.3 (= [1.7+1.2+1.3+1.0+1.4]/5). Note that the ranking of the predicted fatigue life for ALF test lanes has a very good agreement with the measured fatigue performance data.

Step 7: Calculate Fatigue Damage

Using Equation 20, fatigue damage corresponding to a specific number of ALF passes was calculated. Figure 29 shows the relationship between the observed fatigue cracking area (%)

and calculated fatigue damage for each test lane. Note that the calculated damage in Figure 29 is based on the predicted N_f after applying the averaged shift factor of 1.3.

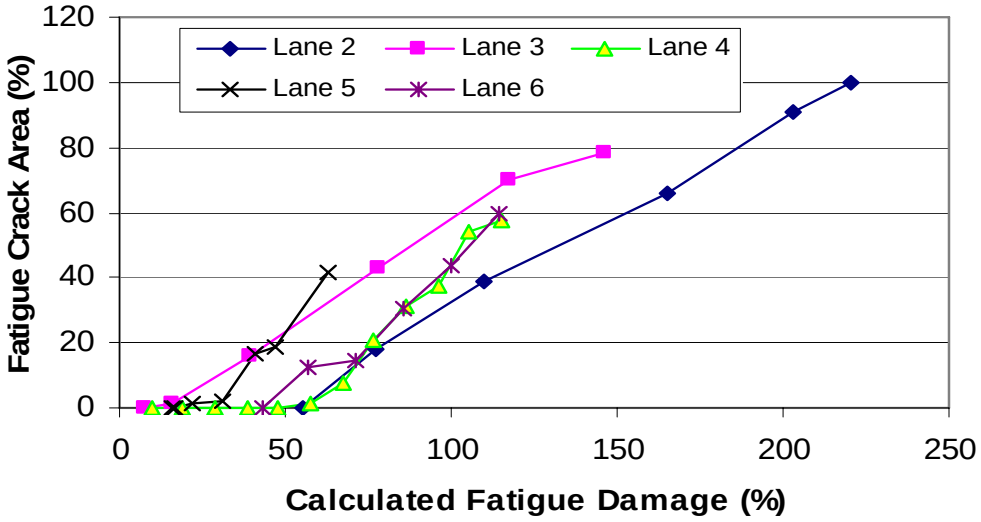

Figure 29. Calculated Fatigue Damage (%) vs. Observed Fatigue Crack Area (%).

Step 8: Predict Fatigue Crack Amount

Using prediction Equations 20, 21, and 22, the fatigue cracking area for each lane was predicted. Since the ALF test lanes 2 to 6 have the same asphalt layer thickness, the constant a_2 was the same for each lane. The calculated a_2 from Equation 22 is –2.8096. Figure 30 shows the predicted fatigue crack amount from the MEPDG Equation 20 for Lanes 2 to 6. For comparison, the observed fatigue crack area vs. calculated fatigue damage is also plotted in Figure 30. It can be seen that the trend of fatigue cracking development predicted from the MEPDG fatigue cracking amount model (Equations 20 to 22) is different from what has been observed in the ALF test lanes. Generally, the MEPDG fatigue crack amount model over predicted fatigue cracking area, when the fatigue damage computed from Equation 19 is below 100 percent. In contrast, the predicted fatigue cracking area is under predicted from the MEPDG model, when the fatigue damage becomes more than 100 percent. Thus, this existing MEPDG fatigue crack amount model needs to be further calibrated.

Since the influence of pavement structure, material properties (modulus, Poisson's ratio, and fracture properties) have been taken into account by fatigue damage, it is reasonable to expect that the parameters a_1 and a_2 in Equation 20 are purely regression constants. With the above known fatigue damage and fatigue crack area data, using Excel's "Solver" optimization

technique, the constants a_1 and a_2 were calibrated in this project. The calibrated a_1 and a_2 are a_1 = 15.78 and a_2 = –7.89. Figure 31 shows the curve fitting results.

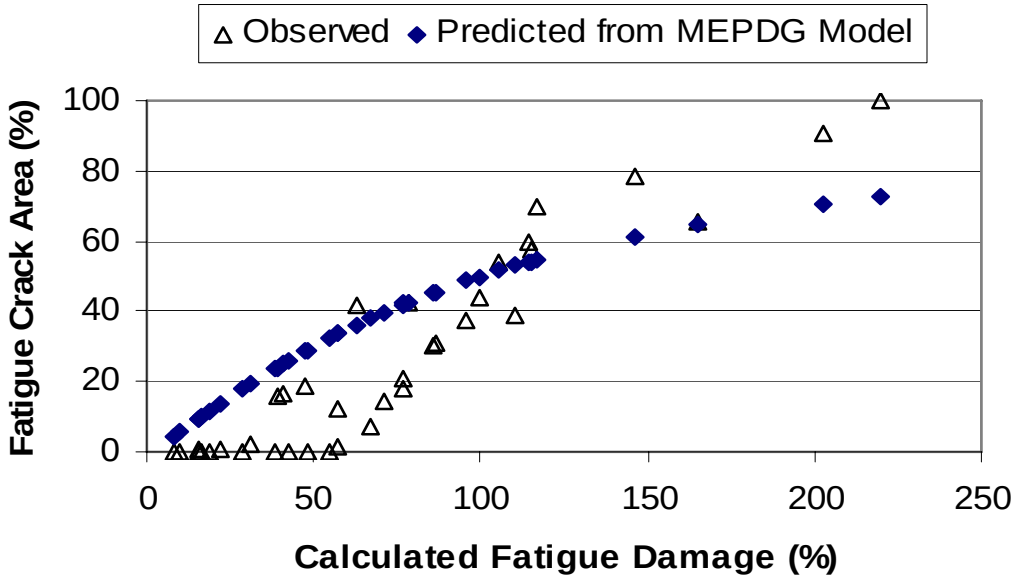

Figure 30. Predicted Fatigue Crack Area (%) from the MEPDG Fatigue Crack Amount Model.

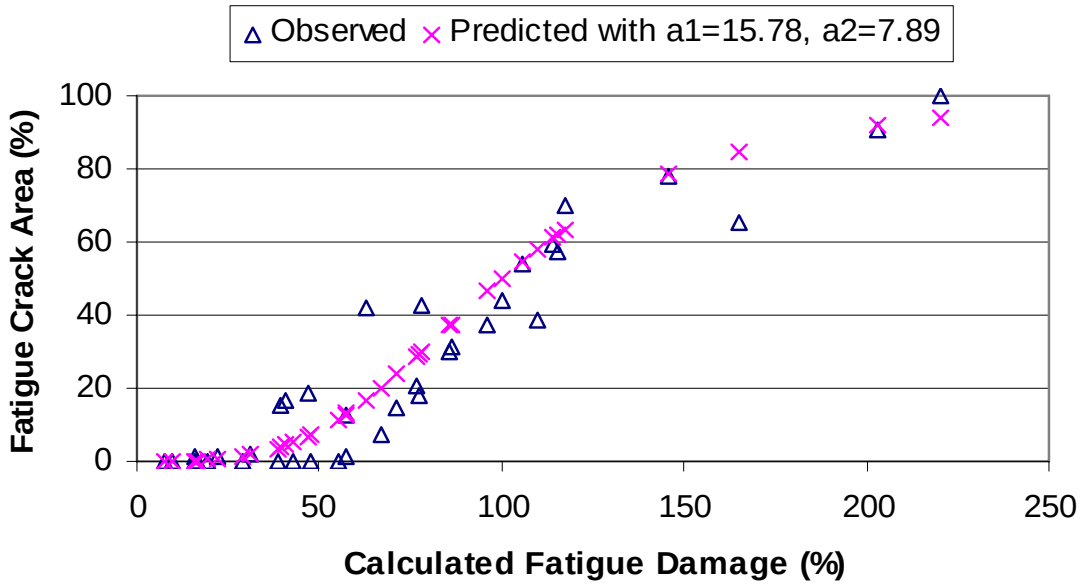

Figure 31. Predicted Fatigue Crack Area (%) from the Calibrated Fatigue Crack Amount Model.

DISCUSSION

Importance of Crack Propagation

Fatigue cracking results from crack initiation and crack propagation. However, most fatigue life prediction models only consider the crack initiation stage. Consequently, a large shift factor is often used to compensate the contributions of crack propagation and other factors (such as healing) to fatigue life. For example, the shift factor (k_1) used in the current MEPDG fatigue life prediction model is presented in Equation 23 and its value ranges for 250 to 2500, as shown in Figure 32 (*1*). By contrast, the averaged shift factor determined from the OT based fatigue crack prediction methodology taking into account both crack initiation and crack propagation is only 1.3. This big difference between the two shift factors clearly indicates the importance of crack propagation to fatigue life. Also, the importance of the OT to characterize the crack propagation stage should also be emphasized.

$$k_1 = \frac{1}{0.000398 + \frac{0.003602}{1 + e^{11.02 - 3.49 h_{ac}}}} \quad (23)$$

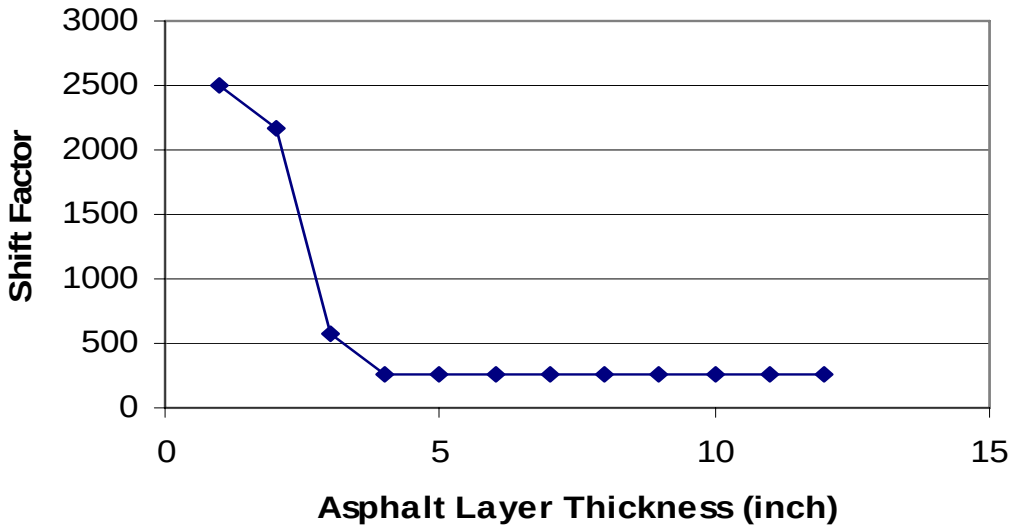

Figure 32. Shift Factors for Fatigue Life Model in the MEPDG.

Implementation of the OT Based Fatigue Crack Prediction Approach

A step-by-step implementation of the proposed OT based fatigue crack prediction approach has been demonstrated in this report. Compared to the traditional fatigue cracking prediction approach, this proposed approach has two more major components for fatigue crack

propagation; the OT testing and calculation of the SIFs (bending and shearing). As noted previously, the OT is a simple, rapid routine test for characterizing fracture properties of HMA mixtures. The associated data interpretation for fracture properties (A and n) of HMA mixtures, as shown previously, is not complicated either. Furthermore, an Excel macro named TTI-OT is under development to automatically determine the fracture properties (A and n).

The calculation of the SIFs (bending and shearing) seems difficult. However, a specific program named *SA-CrackPro* has been developed to automatically calculate the bending and shearing SIFs with growing crack length in this project. The inputs to *SA-CrackPro* program are the same as those used in the multilayer elastic program for calculating tensile strain at the bottom of the asphalt layer. Furthermore, regression equations for bending and shearing SIFs are under development. Once regression equations are developed, the implementation of the proposed approach will become much easier.

SUMMARY

This chapter developed the OT based fatigue cracking prediction approach in which the OT is used to characterize fracture properties of HMA mixtures (A and n), which were developed based on fracture mechanics. This approach considers both crack initiation and crack propagation stages. Therefore, the approach presented is different from traditional fatigue crack approaches (such as the fatigue models used in the MEPDG) in which the fatigue crack propagation stage is not directly considered; it is also different from the often used fracture mechanics approaches in which the fatigue crack initiation stage is often ignored. Additionally, the FHWA-ALF fatigue test results from Lanes 2 to 6 were used to verify and demonstrate this OT based fatigue cracking prediction approach.

CHAPTER 5
CONCLUSIONS AND RECOMMENDATION

Based on the research presented in this report, the following conclusions and recommendation are made:

CONCLUSIONS

- The FHWA-ALF fatigue test results were used to verify the MEPDG fatigue cracking model. It was found that it was necessary to develop a more reasonable fatigue cracking prediction model that utilizes fundamental HMA mixture properties obtained from simple routine laboratory tests rather than time-consuming fatigue tests.
- The methodology for determining fracture properties (*A* and *n*) of HMA mixtures using the OT has been proposed and demonstrated in this report. The features of the OT for fracture properties (*A* and *n*) include 1) specimen size, 2) specimen preparation, and 3) testing time (within 15 minutes).
- Fatigue crack is a two-stage process: crack initiation followed by crack propagation. Crack initiation is closely related to crack propagation. Theoretical derivations clearly indicated that the parameters, k_1 and k_2, of tradition fatigue model ($N_f = k_1\left[1/\varepsilon\right]^{k_2}$) could be estimated from the fracture properties (*A* and *n*). Based on theoretical derivations and experimental data, the quantitative relationships between crack initiation and crack propagation models were developed in this report.
- The OT based fatigue cracking prediction approach has been proposed in this report. Different from the traditional fatigue models focusing on crack initiation, the proposed approach considers both crack initiation and crack propagation. This proposed approach has been successfully verified and demonstrated by analyzing five FHWA-ALF test lanes. The ranking of the predicted fatigue life for ALF test lanes has a very good agreement with the measured fatigue performance data under the ALF loading. Furthermore, these five case studies indicated the significance of crack propagation on the observed fatigue life.

RECOMMENDATION

The results presented in this report are based on a single set of observed pavement performance. The results obtained look very promising. However, the approach presented should be further evaluated on other data sets.

REFERENCES

1. NCHRP, *Guide for Mechanistic-Empirical Design of New and Rehabilitation Pavement Structures*, Transportation Research Board of the National Academics, Washington, D.C., 2004.
2. X. Qi, G. Al-Khateeb, T. Mitchell, K. Stuart, J. Youtcheff, *Determining Modified Asphalt Binder Properties for the Superpave Specification, Report on the Construction of Pavements with Modified Asphalt Binders*, Pooled-Fund Study TPF-5 (019), Jan. 2004.
3. X. Qi, G. Al-Khateeb, A. Shenoy, T. Mitchell, N. Gibson, J. Youtcheff, and T. Harman, Performance of the FHWA's ALF Modified-Binder Pavements, the 10th International Conference on Asphalt Pavement, Quebec, Canada, Aug. 12-17, 2006.
4. X. Qi, T. Mitchell, K. Stuart, J. Youtcheff, K. Petros, T. Harman, and G. Al-Khateeb, Strain Responses in ALF Modified-Binder Pavement Study, *the CD Proceedings of 2nd International Conference on Accelerated Pavement Testing,* Minneapolis, MN, Sept. 2004.
5. MODULUS 6
6. M. Witczak, K. Kaloush, T. Pellinen, M. El-Basyouny, and H. V. Quintus, Simple Performance Test for Superpave Mix Design, NCHRP Report 465, National Research Council, Washington, D.C. 2002.
7. G. Al-Khateeb, A. Shenoy, N. H. Gibson, and T. Harman, A New Simplistic Model for Dynamic Modulus Predictions of Asphalt Paving Mixtures, *Journal of the Association of Asphalt Paving Technologists*, Vol. 75 CD-ROM, 2006.
8. M. M. El-Basyouny and M. Witczak, Calibration of Alligator Fatigue Cracking Model for 2002 Design Guide, Journal of the Transportation Research Board No. 1919, 2005, pp. 77-86.
9. F. P. Germann and R. L. Lytton, *Methodology for Predicting the Reflection Cracking Life of Asphalt Concrete Overlays*, Research Report FHWA/TX-79/09+207-5, College Station, TX, March 1979.
10. D. L. Pickett and R. L. Lytton, *Laboratory Evaluation of Selected Fabrics for Reinforcement of Asphaltic Concrete Overlays*, Research Report 261-1, Texas Transportation Institute, The Texas A&M University System, College Station, TX, August 1983.

11. J. W. Button and J. A. Epps, *Evaluation of Fabric Interlayers*, Research Report 261-2, Texas Transportation Institute, The Texas A&M University System, College Station, TX, November 1982.
12. J. W. Button, J. A. Epps, and R. L. Lytton, *Laboratory Evaluation of Miraf Fabrics for Pavement Overlays*, Research Report 3424-6, for Mirafi Inc., Texas Transportation Institute, The Texas A&M University System, College Station, TX, Jan. 1983.
13. J. W. Button and T. G. Hunter, *Synthetic Fibers in Asphalt Paving Mixtures*, Research Report 319-1F, Texas Transportation Institute, Texas A&M University System, College Station, TX, Jan. 1983.
14. J. W. Button, and R. L. Lytton, Evaluation of Fabrics, Fibers, and Grids in Overlays, *Proceedings of the Sixth International Conference on Structural Design of Asphalt Pavements*, Vol. 1,The University of Michigan, 1987, pp. 925-934.
15. G. S. Cleveland, R. L. Lytton, and J. W. Button, *Reinforcing Benefits of Geosynthetic Materials in Asphalt Concrete Overlays Using Pseudo Strain Damage Theory*, TRB CD, 2003.
16. F. Zhou and T. Scullion, *Overlay Tester: A Rapid Performance Related Crack Resistance Test*, FHWA/TX-05/0-4467-2, Texas Transportation Institute, The Texas A&M University System, College Station, TX, 2005, pp. 85.
17. P.C. Paris and F. Erdogan "A Critical Analysis of Crack Propagation Laws", *Transactions of the ASME, Journal of Basic Engineering*, Series D, 85, No. 3, 1963.
18. R.S. Barsoum, On the Use of Isoparametric Elements in Linear Fracture Mechanics, *International Journal of Numerical Methods in Engineering*, Vol. 10, 1976, pp. 25.
19. H. Tada, P. C. Paris, and G. R. Irwin, *The Stress Analysis of Cracks Handbook*, 3rd Ed., New York, ASME Press, 2000.
20. A.A.A. Molenaar "Structural Performance and Design of Flexible Road Constructions and Asphalt Concrete Overlays", Ph.D. Dissertation, *Delft University of Technology,* 1983.
21. M. M. J. Jacobs, *Crack Growth in Asphaltic Mixes*, Ph. D. Dissertation, Delft University of Technology, Road Railraod Research Laboratory, The Netherlands, 1995.
22. Y. Seo, Y. R. Kim, R. A. Schapery, M. W. Witczak, and R. Bonaquist, A Study of Crack-Tip Deformation and Crack Growth in Asphalt Concrete Using Fracture Mechanics, *Journal of the Association of Asphalt Paving Technologists,* Vol. 73, 2004, pp. 200-228.

23. R. Roque, Z. Zhang, and B. Sankar, Determination of Crack Growth Rate Parameters of Asphalt Mixtures Using the Superpave IDT, *Journal of the Association of Asphalt Paving Technologists,* Vol. 68, 1999, pp. 404-433.
24. R. L. Lytton, J. Uzan, E. G. Fernando, R. Roque, D. Hiltumen, and S. M. Stoffels, *Development and Validation of Performance Prediction Models and Specifications for Asphalt Binders and Paving Mixes*, SHRP A-357, National Research Council, Washington, D.C., 1993.
25. R.A. Schapery "A Theory of Crack Initiation and Growth in Visco-Elastic Media; I: Theoretical Development, II: Approximate Methods of Analysis, III: Analysis of Continuous Growth", *International Journal of Fracture*, Sijthoff and Noordhoff International Publishers, Vol. 11, No. 1, pp.141-159; Vol. 11, No. 3, pp.369-388; and Vol. 11, No. 4, pp.549-562, 1975.
26. S. Erkens, J. Moraal, A. Molenaar, J. Groenendijk, and M. Jacobs, Using Paris' Law to Determine Fatigue Characteristics – A Discussion, *Proceedings of the 8th International Conference on Asphalt Pavements*, Seattle, WA, August 10-14, 1997, pp. 1123-1142.
27. H.J. Lee, Y. R. Kim, and S.W. Lee, Prediction of Asphalt Mix Fatigue Life with Viscoelastic Material Properties, *Journal of the Transportation Research Board*, No. 1832, National Research Council, Washington, D.C., 2003, pp. 139-47.
28. A. Tayebali, et al. *Fatigue Response of Asphalt-Aggregate Mixes*, Report No. SHRP-A-404, Strategic Highway Research Program, National Research Council, Washington D.C., 1994.
29. J. T. Harvey, J. Deacon, B. Tsai, and C. L. Monismith, *Fatigue Performance of Asphalt Concrete Mixes and Its Relationship to Asphalt Concrete Pavement Performance in California*, RTA-65W485-2, Asphalt Research Program, CAL/APT Program, Institute of Transportation Studies, University of California at Berkeley, 1996.
30. J. B. Sousa, J. C. Pais, M. Prates, R. Barros, P. Langlois, and A-M Leclerc, Effect of Aggregate Gradation on Fatigue Life of Asphalt Concrete Mixes, Transportation Research Record, No. 1630, 1998, pp. 62-68.
31. B. Tsai, *High Temperature Fatigue and Fatigue Damage Process of Aggregate-Asphalt Mixes*, Ph.D. Dissertation, University of California at Berkeley, June 2001.
32. K. A. Ghuzlan and S. H. Carpenter, Traditional Fatigue Analysis of Asphalt Concrete Mixtures, Transportation Research Board, CD-ROM, Washington, D.C., 2003.

33. B. Tsai, , J. T. Harvey, and C. L. Monismith, Two-Stage Weibull Approach for Asphalt Concrete Fatigue Performance Prediction, *Journal of the Association of Asphalt Paving Technologists,* Vol. 73, 2004, pp. 200-228.

APPENDIX A
FWD RESULTS FROM FHWA-ALF FATIGUE TEST LANES IN MARCH 2003

Table A1. FWD Data Backcalculation: FHWA-ALF Fatigue Test Lane 2–March 2003.

TTI MODULUS ANALYSIS SYSTEM (SUMMARY REPORT) (Version 6.0)

District:
County :
Highway/Road: FHWA-ALF Lane-2: Fatigue

	Thickness(in)	MODULI RANGE(psi) Minimum	Maximum	Poisson Ratio Values
Pavement:	4.00	850,000	2,480,000	H1: v = 0.38
Base:	22.00	5,000	150,000	H2: v = 0.35
Subbase:	0.00			H3: v = 0.00
Subgrade:	90.43(by DB)	3,000		H4: v = 0.35

Station	Load (lbs)	Measured Deflection (mils): R1	R2	R3	R4	R5	R6	R7	Calculated Moduli values (ksi): SURF(E1)	BASE(E2)	SUBB(E3)	SUBG(E4)	Absolute ERR/Sens	Depth to Bedrock
102.140	16,219	37.91	29.21	23.58	18.66	11.34	6.89	4.80	1862.1	9.8	0.0	7.5	0.14	135.4
106.140	16,155	38.98	30.12	25.16	19.53	11.57	7.01	4.70	2020.0	7.8	0.0	7.8	1.05	134.0
110.140	16,012	40.28	31.50	25.39	19.65	11.69	7.05	4.30	1776.2	8.1	0.0	7.5	0.92	131.3
114.140	15,996	40.71	30.94	25.00	19.33	11.34	6.42	4.50	1693.1	7.8	0.0	8.1	0.40	109.5
118.140	16,044	39.69	30.35	24.88	19.65	11.73	7.32	4.70	1744.9	9.5	0.0	7.0	0.87	150.8
122.140	16,012	38.98	30.43	24.80	19.53	11.85	7.24	4.70	1911.5	8.7	0.0	7.2	0.44	138.1
126.140	15,933	40.20	31.10	25.31	20.00	11.93	6.73	4.20	1964.5	6.9	0.0	8.1	0.47	108.7
Mean:		39.54	30.52	24.87	19.48	11.64	6.95	4.56	1853.2	8.4	0.0	7.6	0.61	129.7

Table A2. FWD Data Backcalculation: FHWA-ALF Fatigue Test Lane 3–March 2003.

TTI MODULUS ANALYSIS SYSTEM (SUMMARY REPORT) (Version 6.0)

District:
County :
Highway/Road: FHWA-ALF Lane 3: Fatigue

	Thickness(in)	MODULI RANGE(psi) Minimum	Maximum	Poisson Ratio Values
Pavement:	4.00	690,000	1,990,000	H1: v = 0.38
Base:	22.00	5,000	150,000	H2: v = 0.35
Subbase:	0.00			H3: v = 0.00
Subgrade:	82.73(by DB)	3,000		H4: v = 0.35

Station	Load (lbs)	Measured Deflection (mils): R1	R2	R3	R4	R5	R6	R7	Calculated Moduli values (ksi): SURF(E1)	BASE(E2)	SUBB(E3)	SUBG(E4)	Absolute ERR/Sens	Dpth to Bedrock
102.140	16,680	47.64	37.36	31.06	24.49	14.45	8.70	5.50	1809.8	6.3	0.0	6.3	0.93	130.4 *
106.140	16,441	57.80	42.40	33.94	25.59	14.37	8.62	5.40	982.8	7.0	0.0	5.7	1.16	127.6
110.140	16,426	58.62	42.40	33.94	25.67	14.61	8.82	5.50	902.5	7.6	0.0	5.4	1.05	130.5
114.140	16,505	55.24	40.67	32.72	25.04	14.33	8.58	5.30	1069.2	7.5	0.0	5.7	0.95	127.2
118.140	16,441	55.31	40.08	32.40	24.61	14.17	8.46	5.20	1012.6	7.8	0.0	5.7	0.98	126.0
122.140	16,457	51.30	37.99	30.75	23.50	13.74	8.31	5.20	1173.8	8.2	0.0	5.9	0.89	132.0
126.140	16,553	49.88	36.93	29.96	22.80	13.19	7.99	5.00	1223.2	8.2	0.0	6.2	1.10	132.9
Mean:		53.68	39.69	32.11	24.53	14.12	8.50	5.30	1167.7	7.5	0.0	5.8	1.01	129.5

Table A3. FWD Data Backcalculation: FHWA-ALF Fatigue Test Lane 4–March 2003.

TTI MODULUS ANALYSIS SYSTEM (SUMMARY REPORT) (Version 6.0)

District:
County :
Highway/Road: FHWA-ALF Lane 4: Fatigue

	Thickness(in)	MODULI RANGE(psi) Minimum	Maximum	Poisson Ratio Values
Pavement:	4.00	890,000	2,990,000	H1: v = 0.38
Base:	22.00	5,000	150,000	H2: v = 0.35
Subbase:	0.00			H3: v = 0.00
Subgrade:	92.42(by DB)	3,000		H4: v = 0.35

Station	Load (lbs)	Measured Deflection (mils): R1	R2	R3	R4	R5	R6	R7	Calculated Moduli values (ksi): SURF(E1)	BASE(E2)	SUBB(E3)	SUBG(E4)	Absolute ERR/Sens	Depth to Bedrock
102.140	16,394	42.05	32.52	27.17	21.34	13.07	8.19	5.30	1848.0	8.6	0.0	6.6	0.85	153.5
106.140	16,298	46.69	35.51	29.21	22.56	13.23	8.07	5.10	1495.3	7.5	0.0	6.7	0.98	136.6
110.140	16,378	45.55	34.72	28.50	22.05	13.07	8.15	5.20	1511.8	8.3	0.0	6.6	1.04	149.6
114.140	16,298	46.93	35.55	29.02	22.44	13.31	8.27	5.30	1401.1	8.3	0.0	6.4	0.92	147.1
118.140	16,267	46.14	34.72	28.70	22.28	13.19	8.11	5.10	1485.1	8.1	0.0	6.5	1.07	141.1
122.140	16,346	45.79	34.84	28.74	22.36	13.15	7.99	5.00	1569.9	7.6	0.0	6.8	0.97	134.8
126.140	16,267	43.78	33.58	27.83	21.61	12.80	7.80	4.90	1684.7	7.7	0.0	7.0	0.91	136.4
Mean:		45.28	34.49	28.45	22.09	13.12	8.08	5.13	1570.8	8.0	0.0	6.7	0.96	142.7

Table A4. FWD Data Backcalculation: FHWA-ALF Fatigue Test Lane 5–March 2003.

TTI MODULUS ANALYSIS SYSTEM (SUMMARY REPORT) (Version 6.0)

District:
County :
Highway/Road: FHWA-ALF Lane 5: Fatigue

	Thickness(in)	MODULI RANGE(psi) Minimum	Maximum	Poisson Ratio Values
Pavement:	4.00	490,000	1,990,000	H1: v = 0.38
Base:	22.00	5,000	150,000	H2: v = 0.35
Subbase:	0.00			H3: v = 0.00
Subgrade:	74.27(by DB)	3,000		H4: v = 0.35

Station	Load (lbs)	Measured Deflection (mils): R1	R2	R3	R4	R5	R6	R7	Calculated Moduli values (ksi): SURF(E1)	BASE(E2)	SUBB(E3)	SUBG(E4)	Absolute ERR/Sens	Depth to Bedrock
102.140	16,155	55.83	41.30	33.31	25.04	14.06	8.39	5.40	1048.8	7.0	0.0	5.4	1.40	125.5
106.140	16,267	55.08	40.63	32.83	24.57	13.74	8.27	5.30	1051.2	7.2	0.0	5.5	1.58	129.3
110.140	16,187	57.76	42.40	33.74	25.08	13.98	8.27	5.30	950.6	6.9	0.0	5.4	1.40	121.9
114.140	16,108	62.87	44.72	35.43	25.98	14.09	8.15	5.20	790.1	6.5	0.0	5.4	1.45	113.8
118.140	16,028	67.09	47.48	37.28	27.72	15.16	8.82	5.40	703.3	6.5	0.0	4.8	1.10	115.5
122.140	16,076	65.51	47.68	38.19	28.66	15.91	9.29	5.50	839.3	6.0	0.0	4.8	1.17	116.9
126.140	16,092	61.81	45.71	37.05	27.87	15.51	8.90	5.40	987.3	5.7	0.0	5.1	1.13	111.8
Mean:		60.85	44.27	35.40	26.42	14.64	8.58	5.36	910.1	6.5	0.0	5.2	1.32	119.2

Table A5. FWD Data Backcalculation: FHWA-ALF Fatigue Test Lane 6–March 2003.

TTI MODULUS ANALYSIS SYSTEM (SUMMARY REPORT) (Version 6.0)

District:
County :
Highway/Road: FHWA-ALF Lane 6: Fatigue

	Thickness(in)	MODULI RANGE(psi) Minimum	Maximum	Poisson Ratio Values
Pavement:	4.00	490,000	1,990,000	H1: v = 0.38
Base:	22.00	5,000	150,000	H2: v = 0.35
Subbase:	0.00			H3: v = 0.00
Subgrade:	92.24(by DB)	3,000		H4: v = 0.35

Station	Load (lbs)	Measured Deflection (mils): R1	R2	R3	R4	R5	R6	R7	Calculated Moduli values (ksi): SURF(E1)	BASE(E2)	SUBB(E3)	SUBG(E4)	Absolute ERR/Sens	Depth to Bedrock
102.140	16,203	46.89	36.10	30.04	23.35	13.82	8.43	5.40	1660.7	6.6	0.0	6.6	1.00	136.6
106.140	16,235	45.28	35.55	29.65	23.15	13.74	8.46	5.40	1827.3	6.5	0.0	6.7	1.07	141.9
110.140	16,235	47.44	36.38	30.28	23.50	13.78	8.62	5.40	1586.9	6.9	0.0	6.4	1.36	142.2
114.140	16,123	46.57	36.38	30.12	23.43	13.82	8.35	5.40	1753.4	6.0	0.0	6.8	0.94	131.9
118.140	16,219	46.50	35.55	29.57	22.76	13.23	8.19	5.20	1603.4	6.9	0.0	6.8	1.38	144.9
122.140	16,171	42.68	33.07	27.48	21.34	12.76	7.99	5.20	1796.8	7.7	0.0	6.9	1.15	152.7
126.140	16,171	41.81	32.17	26.81	20.91	12.56	7.91	5.20	1782.9	8.4	0.0	6.8	1.08	157.1
Mean:		45.31	35.03	29.14	22.63	13.39	8.28	5.31	1715.9	7.0	0.0	6.7	1.14	143.9

APPENDIX B

FWD RESULTS FROM FHWA-ALF FATIGUE TEST LANES IN SEPTEMBER 2003

Table B1. FWD Data Backcalculation: FHWA-ALF Fatigue Test Lane 2–September 2003.

TTI MODULUS ANALYSIS SYSTEM (SUMMARY REPORT) (Version 6.0)

District:
County :
Highway/Road: FHWA-ALF Lane-2: Fatigue

	Thickness(in)	MODULI RANGE(psi) Minimum	Maximum	Poisson Ratio Values
Pavement:	4.00	850,000	2,480,000	H1: v = 0.38
Base:	22.00	5,000	150,000	H2: v = 0.35
Subbase:	0.00			H3: v = 0.00
Subgrade:	90.43(by DB)	3,000		H4: v = 0.35

Station	Load (lbs)	Measured Deflection (mils): R1	R2	R3	R4	R5	R6	R7	Calculated Moduli values (ksi): SURF(E1)	BASE(E2)	SUBB(E3)	SUBG(E4)	Absolute Depth to ERR/Sens	Bedrock
102.140	16,092	49.57	33.62	25.51	18.07	9.72	6.14	4.30	674	11.1	0.0	6.4	2.42	110.7
106.140	16,060	50.16	35.08	26.93	18.94	9.72	5.91	4.30	796	9.0	0.0	6.8	2.88	93.9
110.140	16,092	52.20	35.75	27.24	19.33	10.04	6.06	4.10	714.7	9.3	0.0	6.5	2.24	97.5
114.140	16,155	51.69	35.67	27.36	19.33	10.24	6.22	4.10	730.4	9.6	0.0	6.4	2.32	104.3
118.140	16,123	51.89	36.22	28.50	20.71	11.22	6.65	4.30	822.5	9.1	0.0	5.9	1.70	114.0
122.140	16,092	53.15	37.28	29.02	21.18	11.30	6.61	4.20	812.8	8.6	0.0	6.0	1.54	107.1
126.140	16,028	54.29	37.95	29.41	21.22	11.22	6.54	4.20	778.3	8.3	0.0	6.0	1.73	103.5
Mean:		51.85	35.94	27.71	19.83	10.49	6.30	4.17	761.2	9.3	0.0	7.0	2.12	104.4

Table B2. FWD Data Backcalculation: FHWA-ALF Fatigue Test Lane 3–September 2003.

TTI MODULUS ANALYSIS SYSTEM (SUMMARY REPORT) (Version 6.0)

District:
County :
Highway/Road: FHWA-ALF Lane 3: Fatigue

	Thickness(in)	MODULI RANGE(psi) Minimum	Maximum	Poisson Ratio Values
Pavement:	4.00	690,000	1,990,000	H1: v = 0.38
Base:	22.00	5,000	150,000	H2: v = 0.35
Subbase:	0.00			H3: v = 0.00
Subgrade:	82.73(by DB)	3,000		H4: v = 0.35

Station	Load (lbs)	Measured Deflection (mils): R1	R2	R3	R4	R5	R6	R7	Calculated Moduli values (ksi): SURF(E1)	BASE(E2)	SUBB(E3)	SUBG(E4)	Absolute Depth to ERR/Sens	Bedrock
102.14	15,837	64.76	43.66	33.11	23.39	11.97	6.93	4.6	560.5	7.2	0.0	5.3	1.83	92.5
106.14	15,726	70.00	44.92	33.03	22.87	11.5	6.89	4.6	398.7	7.7	0.0	5.2	2.23	87.8
110.14	15,758	69.76	45.51	33.94	24.02	12.48	7.48	4.8	430.1	7.8	0.0	4.8	1.75	96.6
114.14	15,821	69.21	45.87	34.53	24.53	12.6	7.32	4.8	484.8	7.2	0.0	5.0	1.58	93.3
118.14	15,710	71.89	47.32	35.51	25.04	12.72	7.24	4.6	458.2	6.8	0.0	4.9	1.54	90.2
122.14	15,726	66.54	45.04	34.29	24.49	12.72	7.28	4.6	559.4	6.9	0.0	5.0	1.47	96.7
126.14	15,885	64.49	42.2	31.93	22.87	12.17	7.17	4.6	489.0	8.5	0.0	5.0	1.34	105.4
Mean:		68.09	44.93	33.73	23.89	12.31	7.19	4.7	483.0	7.4	0.0	5..0	1.68	94.6

Table B3. FWD Data Backcalculation: FHWA-ALF Fatigue Test Lane 4–September 2003.

TTI MODULUS ANALYSIS SYSTEM (SUMMARY REPORT) (Version 6.0)

District:
County :
Highway/Road: FHWA-ALF Lane 4: Fatigue

	Thickness(in)	MODULI RANGE(psi) Minimum	Maximum	Poisson Ratio Values
Pavement:	4.00	890,000	2,990,000	H1: v = 0.38
Base:	22.00	5,000	150,000	H2: v = 0.35
Subbase:	0.00			H3: v = 0.00
Subgrade:	92.42(by DB)	3,000		H4: v = 0.35

Station	Load (lbs)	Measured Deflection (mils): R1	R2	R3	R4	R5	R6	R7	Calculated Moduli values (ksi): SURF(E1)	BASE(E2)	SUBB(E3)	SUBG(E4)	Absolute Depth to ERR/Sens	Bedrock
102.140	15,758	62.76	41.34	31.5	22.56	12.05	7.32	4.7	513.3	8.5	0.0	5.3	1.66	106.9
106.140	15,678	65.31	42.17	31.61	22.32	11.69	7.17	4.7	438.7	8.5	0.0	5.3	1.90	99.5
110.140	15,774	62.56	40.98	30.94	22.01	12.05	7.4	4.8	477.2	9.1	0.0	5.2	1.59	118.4
114.140	15,789	64.37	42.68	32.56	23.35	12.6	7.52	4.8	516.8	8.2	0.0	5.2	1.39	111.2
118.140	15,726	65.94	42.40	31.85	22.6	11.89	6.97	4.6	445.5	8.2	0.0	5.4	1.33	101.0
122.140	15,726	66.38	43.74	32.99	23.31	12.09	7.01	4.5	496.4	7.4	0.0	5.5	1.49	96.3
126.140	15,742	65.43	42.87	32.24	22.72	11.73	6.81	4.4	491.0	7.6	0.0	5.6	1.52	95.0
Mean:		64.68	42.31	31.96	22.70	12.01	7.17	4.6	482.7	8.2	0.0	5.4	1.55	104.0

Table B4. FWD Data Backcalculation: FHWA-ALF Fatigue Test Lane 5–September 2003.

TTI MODULUS ANALYSIS SYSTEM (SUMMARY REPORT) (Version 6.0)

District:
County :
Highway/Road: FHWA-ALF Lane 5: Fatigue

	Thickness(in)	MODULI RANGE(psi) Minimum	Maximum	Poisson Ratio Values
Pavement:	4.00	490,000	1,990,000	H1: v = 0.38
Base:	22.00	5,000	150,000	H2: v = 0.35
Subbase:	0.00			H3: v = 0.00
Subgrade:	74.27(by DB)	3,000		H4: v = 0.35

Station	Load (lbs)	Measured Deflection (mils): R1	R2	R3	R4	R5	R6	R7	Calculated Moduli values (ksi): SURF(E1)	BASE(E2)	SUBB(E3)	SUBG(E4)	Absolute Depth to ERR/Sens	Bedrock
102.140	15,646	73.66	48.66	36.18	24.92	12.48	7.13	4.8	435.6	6.5	0.0	4.9	2.08	86.7
106.140	15,662	70.51	46.65	35.16	24.76	12.8	7.52	5.0	461.2	7.2	0.0	4.7	1.84	95.0
110.140	15,678	71.10	47.01	35.04	24.53	12.76	7.44	4.9	442.2	7.2	0.0	4.7	1.72	96.8
114.140	15,662	74.92	49.09	36.57	25.59	12.95	7.44	4.9	419.6	6.6	0.0	4.7	1.73	89.1
118.140	15,599	76.73	50.43	37.72	26.57	13.50	7.60	5.0	420.1	6.4	0.0	4.5	1.39	90.0
122.140	15,487	79.96	54.21	40.94	28.94	14.53	8.03	5.1	464.8	5.3	0.0	4.4	1.49	87.0
126.140	15,519	80.28	53.54	40.39	28.15	14.06	7.56	4.8	439.4	5.4	0.0	4.5	1.36	85.8
Mean:		75.31	49.94	37.43	26.21	13.30	7.53	4.9	440.4	6.4	0.0	4.6	1.66	90.1

Table B5. FWD Data Backcalculation: FHWA-ALF Fatigue Test Lane 6–September 2003.

TTI MODULUS ANALYSIS SYSTEM (SUMMARY REPORT) (Version 6.0)

District:
County :
Highway/Road: FHWA-ALF Lane 6: Fatigue

	Thickness(in)	MODULI RANGE(psi) Minimum	Maximum	Poisson Ratio Values
Pavement:	4.00	490,000	1,990,000	H1: v = 0.38
Base:	22.00	5,000	150,000	H2: v = 0.35
Subbase:	0.00			H3: v = 0.00
Subgrade:	92.24(by DB)	3,000		H4: v = 0.35

Station	Load (lbs)	Measured Deflection (mils): R1	R2	R3	R4	R5	R6	R7	Calculated Moduli values (ksi): SURF(E1)	BASE(E2)	SUBB(E3)	SUBG(E4)	Absolute Depth to ERR/Sens	Bedrock
102.140	15,487	78.43	50.24	36.85	25.28	12.24	6.77	4.5	369.8	6.2	0.0	4.8	1.83	79.9
106.140	15,535	76.57	50.43	37.2	25.43	12.36	6.93	4.6	414.0	6.0	0.0	4.9	2.23	80.6
110.140	15,535	77.87	51.14	37.2	25.51	12.36	7.05	4.7	389.8	6.1	0.0	4.8	2.38	80.0
114.140	15,599	76.97	50.55	36.97	25.43	12.24	6.77	4.5	410.8	6.0	0.0	5.0	1.96	78.9
118.140	15,599	75.71	49.29	35.87	24.33	11.93	6.77	4.6	387.7	6.5	0.0	5.0	2.36	82.2
122.140	15,662	70.63	46.3	34.06	23.43	11.81	6.97	4.9	420.2	7.3	0.0	4.9	2.40	88.3
126.140	15,662	69.06	45.04	33.07	22.83	11.54	6.77	4.7	423.2	7.5	0.0	5.1	2.17	89.0
Mean:		75.00	49.00	35.90	24.60	12.10	6.90	4.6	402.2	6.5	0.0	4.9	2.20	82.7

APPENDIX C
FRACTURE MECHANICS APPROACH VS. TRADITIONAL FATIGUE APPROACH

Fatigue cracking is the result of a crack initiation process followed by a crack propagation process. Therefore, the number of traffic load cycles (N_f) to cause a crack to propagate through the full depth of the surface layer is the sum of the number of load cycles for micro-cracks to coalesce to initiate a macro-crack (N_i) and the number of load cycles required for the macro-crack to propagate to the surface (N_p).

$$N_f = N_i + N_p \qquad \text{(C1)}$$

As noted by Lytton et al., in the crack initiation stage, the growth of micro-cracks obeys the same fracture law as do the visible cracks in the macro-crack propagation stage (*1*). The fundamental fracture law is the well-known Paris' law, which is shown in Equation C2 (*2*).

$$\frac{dc}{dN} = A(\Delta K)^n \qquad \text{(C2)}$$

where:

c = crack length,
N = number of load cycles,
dc/dN = crack speed or rate of crack growth,
ΔK = change of stress intensity factor (SIF), and
A, n = fracture properties of material.

Note that the computed, dimensionless SIF (K) is a function of a dimensionless crack length, of the form (*1*),

$$\frac{K}{\sigma\sqrt{d}} = r\left(\frac{c}{d}\right)^q \qquad \text{(C3)}$$

where:

d = layer thickness,
σ = E*ε = maximum stress in the specimen,
E = elastic stiffness corresponding to a specific loading frequency and temperature,
ε = maximum strain in the specimen,
c = crack length, and
r, q = regression coefficients.

Integrating the Paris' law, Lytton et al. produced the following expression (*1*):

$$N_p = \frac{d^{\left(1-\frac{n}{2}\right)}}{A r^n (1-nq) E^n}\left[1-\left(\frac{c_0}{d}\right)^{(1-nq)}\right]\left(\frac{1}{\varepsilon}\right)^n \qquad \text{(C4)}$$

where:

c_0 = initial crack length.

It is apparent that the above equation for cracking propagation is of the same form as the traditional fatigue equation developed based on strain-controlled tests that mainly characterize crack initiation stage:

$$N_i = k_1\left(\frac{1}{\varepsilon}\right)^{k_2} \qquad \text{(C5)}$$

In general, the traditional fatigue cracking prediction approach, which ignores the crack propagation, often takes N_i in Equation C5 as N_f. Similarly, the fracture mechanics approach in which the crack initiation is often neglected, generally takes N_p in Equation C4 as N_f. This means that Equation C4 can be equated to Equation C5. Thus, the constants, k_1 and k_2, of the traditional fatigue equation can be calculated from the following expressions:

$$k_1 = \frac{d^{\left(1-\frac{n}{2}\right)}}{A r^n (1-nq) E^n}\left[1-\left(\frac{c_0}{d}\right)^{(1-nq)}\right] \qquad \text{(C6)}$$

$$k_2 = n \qquad \text{(C7)}$$

REFERENCE

1. R.L. Lytton, J. Uzan, E.G. Fernando, R. Roque, D. Hiltumen, and S.M. Stoffels, *Development and Validation of Performance Prediction Models and Specifications for Asphalt Binders and Paving Mixes*, SHRP A-357, National Research Council, Washington, D.C., 1993.
2. P.C. Paris and F. Erdogan, A Critical Analysis of Crack Propagation Laws, *Transactions of the ASME, Journal of Basic Engineering*, Series D, 85, No. 3, 1963.

APPENDIX D

CONTINUUM DAMAGE MECHANICS APPROACH VS. TRADITIONAL FATIGUE APPROACH

Continuum damage theory was originally developed by R.A. Schapery for analyzing the response of solid rocket fuels and similar viscoelastic materials (*1, 2, 3*). Lytton, Kim, and Little later applied Schapery's work to asphalt concrete (*4*). Their work was extended and refined by Y. Richard Kim, Lee, Daniel, and Yong-Rak Kim (*5, 6, 7, 8, 9, 10*). Practical application of this continuum damage theory has been made by Lee et al. (*10*), and Christensen et al. (*11*). The brief discussion presented below largely follows the development of Christensen et al. (*11*).

Schapery defined uniaxial pseudo-strain as follows:

$$\varepsilon^R(t) = \frac{1}{E_R}\int_0^t E(t-t')\frac{\partial \varepsilon}{\partial t'}dt' \qquad \text{(D1)}$$

where:

ε = strain,

$\varepsilon^R(t)$ = pseudo-strain at time t,

E = relaxation modulus,

t′ = time at which loading begins, and

E^R = an arbitrary reference modulus, often set at unity.

The above definition is very similar to that for linear viscoelastic (LVE) stress:

$$\sigma(t) = \int_0^t E(t-t')\frac{\partial \varepsilon}{\partial t'}dt' \qquad \text{(D2)}$$

where:

$\sigma(t)$ = stress at time t.

From Equations D1 and D2, under LVE conditions, we have:

$$\varepsilon^R(t) = \frac{\sigma(t)}{E_R} \qquad \text{(D3)}$$

That means that the pseudo-strain is equal to the stress resulting from an applied strain history. To quantify damage accumulation, Kim et al. used the concept of pseudo-stiffness (*8*):

$$C = \frac{\sigma_{max}}{\varepsilon^R_{max}} \qquad \text{(D4)}$$

where:

C is the normalized pseudo-stiffness; normalization meaning that adjustments are made in the calculation of *C* for individual specimens so that the initial value (undamaged) is always unity.

For fatigue testing, a specimen is subjected to a given strain-controlled loading. With the damage accumulating during the fatigue test, the resulting stress σ_{max} for every cycle will gradually decrease compared to the pseudo-strain. Thus, Equation 4 simply defines pseudo-stiffness as the ratio of the non-linear stress to the linear stress (or the non-linear modulus to the initial LVE modulus). The constitutive equation for uniaxial loading of a viscoelastic material with damage is given below (*11*):

$$\sigma_{max} = C\varepsilon_{max}^{R} \tag{D5}$$

The applicable stress-pseudo-strain relationship is as follows (*11*):

$$\sigma_{max} = \left(\frac{\partial W^{R}}{\partial \varepsilon_{max}^{R}}\right)^{\alpha} \tag{D6}$$

where:

W^R is the pseudo-strain energy density function. The time dependent growth of damage can be given by the following equation (*11*):

$$\frac{dS}{dt} = \left(-\frac{\partial W^{R}}{\partial S}\right)^{\alpha} \tag{D7}$$

where:

S is a variable characteristic of the amount of internal damage in a material, and α is a material constant, which usually has a value close to 2.0. Equations D5 and D6 can be combined and integrated to yield the following relationship (*11*):

$$W^{R} = 0.5C\left(\varepsilon_{max}^{R}\right)^{2} \tag{D8}$$

Regarding the relationship between pseudo-stiffness *C* and the internal damage parameter *S*, Lee and Kim proposed a form of generalized power law (*7*):

$$C = C_{10} - C_{11}(S)^{C_{12}} \tag{D9}$$

where:

C_{10}, C_{11}, and C_{12} are constants describing the rate of damage accumulation of a specimen under cyclic loading. It should be noted that this equation would become negative at some value of *S*, which means that the damaged modulus would also be negative, and an applied tensile

strain would result in a compressive stress. Knowing the limitation of Equation D9, Christensen and Banoquist suggested a better function in a simple exponential form *(11)*:

$$C = \exp(C_2 S) \tag{D10}$$

where:

C_2 is a constant indicative of the rate of damage accumulation in a specimen under cyclic loading. Now, substitute Equation D10 into Equation D8, and differentiate with respect to S; the following relationship results:

$$\frac{\partial W^R}{\partial S} = 0.5 C_2 \exp(C_2 S)\left(\varepsilon^R_{max}\right)^2 \tag{D11}$$

Then, substitute Equation D11 into Equation D7 and integrate to solve for t:

$$t = \frac{2^\alpha \exp(-\alpha C_2 S)}{\alpha(-C_2)^{1+\alpha}\varepsilon^R_{max}}\Bigg|_{S=0}^{S=t} \tag{D12}$$

Now, if the reference modulus $E^R = 1$, then, $\varepsilon^R(t) = \sigma(t)$. In addition, for sinusoidal loading, the maximum tensile stress is equal to:

$$\frac{|\sigma_{max} - \sigma_{min}|}{2} = \sigma_0 = \varepsilon_0 \times |E|_{LVE} \tag{D13}$$

where:

$|E|_{LVE}$ = LVE complex modulus,

σ_0 = maximum tensile stress (or stress amplitude), and

ε_0 = maximum tensile strain (or strain amplitude).

Note that the number of loading cycles N is loading time t times frequency f (*Hz*). Equation D11 can then be solved over the given integration limits and given in the following form:

$$N = \frac{2^\alpha f\left[\exp(-\alpha C_2 S_f) - 1\right]}{\alpha(-C_2)^{1+\alpha}\varepsilon_0^{2\alpha}|E|^{2\alpha}_{LVE}} \tag{D14}$$

where:

S_f is the value of internal damage variable S at failure. The value of S as a function of time may be obtained using experimentally measured data by the following form:

$$S(t) \cong \sum_{i=1}^{N}\left[0.5\left(\varepsilon^R_{mi}\right)^2 (C_{i-1} - C_i)\right]^{\frac{\alpha}{1+\alpha}} (t_i - t_{i-1})^{\frac{1}{1+\alpha}} \tag{D15}$$

Substitute Equation D10 into Equation D14, and we have:

$$N = \frac{2^{\alpha} f\left(C^{-\alpha} - 1\right)}{\alpha\left(-C_2\right)^{1+\alpha} \left|E\right|_{LVE}^{2\alpha}} \left(\frac{1}{\varepsilon_0}\right)^{2\alpha} \tag{D16}$$

The above equation can be expressed in the following form:

$$N = k_1 \left(\frac{1}{\varepsilon_0}\right)^{k_2} \tag{D17}$$

where:

$$k_1 = \frac{2^{\alpha} f\left(C^{-\alpha} - 1\right)}{\alpha\left(-C_2\right)^{1+\alpha} \left|E\right|_{LVE}^{2\alpha}} = f * \text{function}\left(\alpha, \left|E\right|_{LVE}, f, C, C_2\right) \tag{D18}$$

$$k_2 = 2\alpha \tag{D19}$$

For fatigue analysis (or fatigue test), both frequency *f* and the pseudo stiffness *C* are known parameters (e.g., *C*=0.5). As stated by Christensen and Banoquist, C_2 is a function of mixture modulus, voids filled with asphalt (*VFA*), design compaction (i.e., N_{design}), relative density, and binder rheological index *R* (*11*). For simplicity, Equation D18 can be expressed in the following form:

$$\log k_1 = a_1 + a_2 k_2 + a_3 \log\left|E\right|_{LVE} \tag{D20}$$

The main advantage of using continuum damage mechanics to predict fatigue behavior of HMA mixes is that the time-temperature superposition principle can be employed to shift the characteristic curve determined at one temperature to different temperatures. In that way, it is possible to save considerable time and materials. The disadvantage of this approach is that it needs sophisticated data analysis.

REFERENCES

1. R.A. Schapery, A Theory of Mechanical Behavior of Elastic Media with Growing Damage and Other Changes in Structure, *J. Mech. Phys. Solids*, Vol. 38, 1990, pp. 215-253.
2. R.A. Schapery, On Viscoelastic Deformation and Failure Behavior of Composite Materials with Distributed Flaws, *Advances in Aerospace Structures and Materials*, AD-01, ASME, New York, NY,1981, pp. 5-20.
3. R.A. Schapery, "Correspondence Principles and a Generalized J-Integral for Large Deformation and Fracture Analysis of Viscoelastic Media," *Int. J. Fract*., Vol. 25, 1984, pp. 195-223.
4. D.N. Little, R.L. Lytton, D. Williams, C.W. Chen, and Y.R. Kim, "Fundamental Properties of Asphalts and Modified Asphalts—Task K: Microdamage Healing in Asphalt and Asphalt Concrete," FHWA Final Report, Vol. 1, Report No. DTFH61-92-C-00170, Springfield, VA: National Technical Information Service, 1997.
5. H.J. Lee, *Uniaxial Constitutive Modeling of Asphalt Concrete Using Viscoelasticity and Continuum Damage Theory*, Ph.D. Dissertation, North Carolina State University, Raleigh, NC, 1996.
6. Y.R. Kim, H.J. Lee, and D.N. Little, "Fatigue Characterization of Asphalt Concrete Using Viscoelasticity and Continuum Damage Theory," *Journal of the Association of Asphalt Paving Technologists*, Vol. 66, 1997, pp. 520-569.
7. H.J. Lee, and Y.R. Kim, "A Uniaxial Viscoelastic Constitutive Model for Asphalt Concrete Under Cyclic Loading," *ASCE Journal of Engineering Mechanics*, Vol. 124, 1998, No. 11, pp. 1224-1232.
8. Y.R. Kim, D.N. Little, and R.R. Lytton, "Use of Dynamic Mechanical Analysis (DMA) to Evaluate the Fatigue and Healing Potential of Asphalt Binders in Sand Asphalt Mixtures," *Journal of the Association of Asphalt Paving Technologists*, Vol. 71, 2002, pp. 176-199.
9. J.S. Daniel, and Y.R. Kim, "Development of a Simplified Fatigue Test and Analysis Procedure Using a Viscoelastic, Continuum Damage Model," *Journal of the Association of Asphalt Paving Technologists*, Vol. 71, 2002, pp. 619-645.
10. H.J. Lee, Y.R. Kim, and S.W. Lee, Prediction of Asphalt Mix Fatigue Life with Viscoelastic Material Properties, *Journal of the Transportation Research Board*, No. 1832, 2003, pp.139-147.

11. D. Christensen, Jr. and R. Bonaquist, Practical Application of Continuum Damage Theory to Fatigue/Phenomena in Asphalt concrete Mixtures, *Journal of the Association of Asphalt Paving Technologists*, Vol. 74, 2005, pp. 963-1001.